THE EFFECT OF CARBOXYLIC ACIDS ON THE SIZE AND SHAPE OF Co_3O_4 NANOPARTICLES: USED AS CAPPING MOLECULES AND LIGANDS IN THE PREPARATION METHOD

DISSERTATION BY:

P.M. THABEDE (214026582)

SUBMITTED IN PARTIAL FULFILMENT OF THE REQUIREMENT FOR THE DEGREE MAGISTER TECHNOLOGIAE IN THE

DEPARTMENT OF CHEMISTRY

FACULTY OF APPLIED AND COMPUTER SCIENCES

AT THE

VAAL UNIVERSITY OF TECHNOLOGY

SUPERVISOR: DR. E.L VILJOEN

CO-SUPERVISOR: PROF M.J. MOLOTO

ACADEMIC YEAR 2017

DECLARATION

I hereby declare that the work on "The effect of carboxylic acids on the size and shape of Co_3O_4 nanoparticles: used as capping molecules and ligands in the preparation method" is my own work and it has never been researched before. All materials used have been referenced.

P.M. Thabede (214026582)

……Date ……

Supervisor: DR. E.L Viljoen

…….. Date……..

ACKNOWLEDGEMENTS

I would like to pass my gratitude and thank the people who helped me during the course of completing this project: Vaal University of Technology for accepting my application to further my studies. I would like to thank my husband (Nicholas Muzuthini Thabede) for his understanding, support emotionally and financially and agreeing to further my studies. Many thanks to my mother and my sisters (Refilwe Nkwane and Bahupileng Masike) who supported me and believed in me throughout the years of studying. Prof E B Naidoo for his contribution in making sure I complete the project. Prof M J Moloto for his input, guidance, patience and for being my co-supervisor. To my supervisor Dr. E L Viljoen, I say thank you for being my supervisor and tolerating me. My sincere gratitude to Dr. P K Mubiayi for input, contributions, and in making sure that I complete the dissertation. Dr. P Nyamukamba for always willing to help when requested. Ms. T Xaba for always availing herself when the need arises. Mr. P Ngoy for making sure the instruments are available for characterization and in good condition and for allowing using the instruments whenever there is availability. Thank you to Ms. D S More for giving ideas and valuable input. I would like to send my gratitude to the University of the Witwatersrand (Wits) for characterization of XRD analyses. A special thank you to Ms. Machogo for conducting the XRD analyses. A big thank you to Prof N Moloto for agreeing for XRD analyses to be conducted. NCAP research group for contributing and making a good working environment. Lastly I would like to thank National Research Fund (NRF) for making it possible to complete my work by funding my research.

CONFERENCES AND PUBLICATION

1. South African Chemical Institute (SACI) Inorganic Chemistry Conference. Presented the Flash talk and a poster presentation, "The effect of acetate ions during the preparation of Co_3O_4 nano-cubes and nano-spheres". Rhodes University, Grahamstown, 28 June to 02 July 2015.

2. Nanoscience Young Researchers Symposium (NYRS). Flash talk presentation titled: "Preparation of Co_3O_4 nano-cubes with sizes smaller than 10 nanometers". UNISA Science campus, Gauteng, 9 October 2015.

3. 42nd National Convention of the South African Chemical Institute (SACI) Conference. Presented a poster presentation, "Preparation of Co_3O_4 nano-cubes and nano-spheres". Elangeni Hotel, Durban, 29 November to 4th December 2015.

Publication

EL Viljoen, MJ Moloto, PM Thabede. The effect of acetate ions presents during the preparation on the shape of Co_3O_4 nanoparticles. Digest Journal of Nanomaterials and Biostructures (DJNB) –Vol 12, No.2, April-June 2017. p 571-577.

ABSTRACT

This study reports the synthesis and characterization of cobalt oxide nanoparticles using a microwave technique and chemical precipitation with oxidation method. Cobalt complexes were prepared using carboxylic acids (acetic acid, heptanoic acid, and stearic acid) as ligands. The complexes were characterized by Fourier Transform Infrared Spectroscopy (FTIR), Thermogravimetric Analysis (TGA) and Elemental analyses (EA). Cobalt oxide nanoparticles were synthesized from the complexes via a microwave-assisted technique. A precipitation oxidation preparation reaction was used varying different parameters like pH, time, oxidising agent, heating method and cobalt precursor. The use of the cobalt nitrate and cobalt acetate as cobalt precursors resulted in spherical and cubic nanoparticles respectively. Cobalt precursors containing a longer hydrocarbon chain length, for instance cobalt heptanoate, did not yield cobalt oxide nanoparticles with the precipitation oxidation reaction due non- solubility of the complex. Using cobalt acetate as precursor, an increase in the pH from 7.91 to 10.18 caused the cobalt oxide nanoparticles shape to become well defined cubes with a narrower size range and CoOOH needles formed when the pH was further increased to 12.26. The optimum pH of 10.18 yielded cubic cobalt oxide particles having an average size of 25.45 nm with a standard deviation of 6.12. The nanoparticle size decreased from 35.70 nm to 4.45 nm when the oxygen oxidant was replaced with hydrogen peroxide. Conventional heating with a hotplate yielded nanoparticles with a more homogenous shape and size than microwave heating. The size of the nanoparticles increased from 22.81 nm to 25.45 nm when reaction time changed from 16 hours to72 hours.

TABLE OF CONTENTS

LIST OF ABBREVIATIONS

a.u - Arbitrary units

CTAB-Cetyltrimethyl ammonium bromide

DTA-Differential thermal analyses

EA - Elemental Analyses

fcc-Face centred cubic

FTIR - Fourier transform infrared spectroscopy

JCPDS- Joint Committee on Power Diffraction Standards

mL-Millilitre

M-moles per litre

nm – Nanometre

PL - Photoluminescence

rpm- Revolutions per minute

TEM - Transmission electron microscopy

TGA - Thermogravimetric analyses

UV-vis - Ultraviolet-visible

XRD - X-ray diffraction

LIST OF FIGURES

DISSERTATION OUTLINE

Chapter 1: This chapter covers the outline of the dissertation, introduction, literature review, problem statement, aim and objectives and motivation.

Chapter 2: The purpose of this chapter is to outline the details on materials, chemical reagents, equipment and methods used to synthesize nanoparticles.

Chapter 3: This chapter outlines the results and discussion for the synthesized nanoparticles using all techniques and different conditions of synthesis.

Chapter 4: This chapter summarizes the findings and concludes on research work. It also covers recommendations to be followed emanating from this research.

CHAPTER 1: INTRODUCTION AND LITERATURE REVIEW

1.1 Introduction and Literature Review

Nanotechnology is the science of very small materials which is used to manipulate matter on a very small scale of 1-100 nm (Ozkaya *et al*. 2009). In nanotechnology when the material is very small between 1-100 nm its surface area may increase and the surface reactivity will also increase which are both related to quantum-related effects (Rahdar 2013). The physical and chemical properties of nanomaterials are usually different from the larger bulk form of their material. Over the past years, many researchers have been investigating and trying to understand the nature of nanomaterials (Song *et al*. 2005). The increased interest in these nanomaterials is due to their optical, catalytic and magnetic properties that typically superior compared to the bulk counterpart (Ba-Abbad *et al*. 2012). The optical, catalytic and magnetic property of nanoparticles depends on their size and shape (Teng *et al*. 2010). This is because the structure, shape, and size of a nanocrystallite influence their catalytic activity (Jin *et al*. 2015). It is, therefore, important to prepare crystallites of different shapes and sizes. A decrease in crystallite size suggests that the activity of that catalyst will increase (Fischer *et al*. 2011). In the synthesis of nanoparticles, it is very important to control, not only the particle size but also the morphology and particle size distribution because they may have an influence on their properties. However, particles that are too small can reduce the activity (Bezemer *et al*. 2006). The synthesis of metal nanomaterials has been widely reported by researchers.

There are different types of cobalt oxides namely, CoO_2, Co_2O_3, CoO(OH), Co_3O_4 and CoO (Tang et *al*. 2008). The most forms of stable cobalt oxide are Co_3O_4 and CoO. Cobalt oxyhydroxide, CoO(OH) is a hexagonal structure where a divalent metal cation is situated at an octahedral site and coordinated by six hydroxyl oxygen which can be used in rechargeable alkaline batteries (Tang *et al*. 2008). Chen *et al*. (2016) mentioned that CoOOH is an active material used in conjunction with nickel hydroxide in Ni–H cells. It is non-stoichiometric and the Co has an oxidation state (+3) whilst Co_3O_4 oxidation states are +4, +3, +2 (Chen *et al*. 2016). CoO is an antiferromagnetic material whose magnetic properties and application of gas sensors have been studied. Co_3O_4 displayed high catalytic activity in the CO oxidation (Xie *et al*. 2009). Cobalt oxide (Co_3O_4) is a type of nanomaterial that has gained attention in recent years due to their chemical and physical properties which differ from their bulk properties. Co_3O_4 is a p-type semiconductor with the band gap energy of 1.48 and 2.19 eV (Niasari *et al*. 2009). It belongs to the spinel structure with the cubic packing of oxide ions in which Co(II) ion occupies the tetrahedral sites and Co(III) ions occupying the octahedral sites (Tang *et al*. 2008). Due to some applications such as lithium batteries (Pan *et al.* 2014), catalysis (Hu *et al*. 2010), sensors (Elhag *et al*. 2014), there has been a growing interest in these nanomaterials (Sun *et al*. 2013). The preparation methods have an influence on the size and shape of the nanoparticles. Different preparation methods have been used to get a wider variety of shapes. Some of the methods which have been used are; chemical precipitation reported by Agilandeswari & Kumar (2014), thermal decomposition by Manigandan *et al*. (2013), microwave irradiation was investigated by Babu *et al*. (2014) and hydrothermal process was used by Feng *et al.* (2014), which are outlined fully in sub-section 1.3. In this study, the synthesis of cobalt oxide nanoparticles was obtained by microwave irradiation and chemical precipitation with oxidation method. The microwave is based on the efficiency of the interaction of molecules in a reaction mixture (substrates, catalyst, and solvents) with

electromagnetic wave generated (Soltani *et al*. 2012). Chemical precipitation is based on the hydrolysis mixture of the divalent (Co^{2+}) and trivalent (Co^{3+}) ions (Mascolo *et al*. 2013). The (Co^{2+}) and (Co^{3+}) ions are precipitated in an alkaline medium such as sodium hydroxide, ammonium hydroxide or potassium hydroxide (Mascolo *et al*. 2013). In this research work, the intent species is Co_3O_4 due to its noticeable advantages which arise from theoretical capacity, environmental friendliness, low cost, excellent catalytic property and high corrosion stability (Hou *et al.* 2014). It is, therefore, important to prepare Co_3O_4 nanoparticles that can be used as catalysts.

1.1.1 The effect of size and shape of nanoparticles on catalytic activity

Particles with the same chemical composition but different shapes can have different properties (Pal & Chauhan 2010). The properties of nanoparticles do not only depend on the size but also on the morphology (Pal & Chauhan 2010), for example, catalytic performance depends on shape and size (Xie & Shen 2009). Examples will be discussed to show the effect of the shape and size on the properties**.** Piumetti *et al.* (2013) mentioned that as the crystallite size of the metal decreases, the surface area will increase. Figure 1 illustrates this phenomenon. Hence small nanoparticles are more reactive than larger ones.

Catalytic performance is very sensitive to the particle size because the structural and electronic properties change at the nanoscale level (Xie & Shen 2009). Metal oxides and metal with different shapes will have different catalytic activities (Xie & Shen 2009). Xie & Shen (2009) found that Co_3O_4 nanorods had a higher activity than truncated octahedral nanoparticles for carbon monoxide oxidation. The activity of nanoparticles can be maximized by controlling the morphology (Xiao & Qi 2010, Lee *et al.* 2011). Hence different methods are used to prepare nanoparticles because their ultimate application and performance depend on their shape and size.

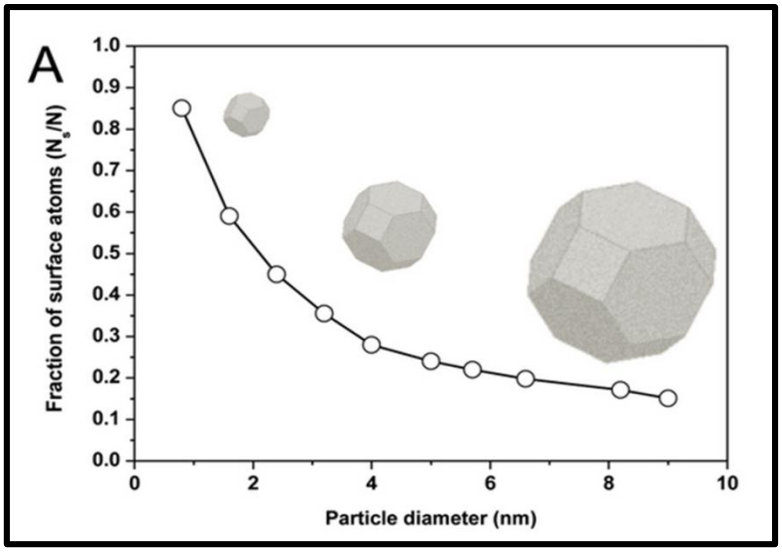

Figure 1: Estimated fractions of surface atoms (Ns/N), where Ns and N are the total numbers of surface atoms and the total number of atoms, respectively, for different metal nanoparticle sizes (Piumetti *et al*. 2013).

1.1.2 Preparation methods of nanoparticles with different sizes and shapes

The properties of nanomaterials including stability, size, and shape are strongly affected by experimental conditions. Because of unique properties, many researchers have made efforts to investigate the dependence of properties on size and shape. Several techniques have been used to synthesize the nanomaterials and some of the preparation methods are discussed in sections below.

1.1.2.1 Microemulsion technique

Microemulsion is macroscopically homogenous, isotropic and thermodynamically stable solutions containing water, oil, and surfactant (Malik *et al*. 2012). The surfactant molecules form an extra layer separating the water and the oil. Particles made using this technique produced have the ability to produce a narrow size distribution (Mohapatra & Anand 2010). However, despite the use of surfactants this method causes aggregation, hence several washing steps are required including further stabilization treatment (Mohapatra & Anand 2010). Microemulsion requires very strict low temperatures of 10-20 °C (Malik *et al*. 2012). Andal & Buvaneswari (2017) synthesized copper nanoparticles by converting copper (I) oxide using hydrazine as a reducing agent. The use of the reducing showed that the copper nanoparticles had low stability because the nanoparticles undergo oxidation under ambient temperature.

1.1.2.2 Thermal decomposition method

Thermal decomposition is the decomposition caused by heat whereby a substance decomposes at a certain temperature to break chemical bonds in the compound. Thermal decomposition is one of the methods to produce stable monodispersed magnetic nanoparticles (Simeonidis *et al.* 2007). The nucleation takes place when the metal precursor is added to a heated solution in the presence of a capping agent. Then the growth stage takes place at a higher reaction temperature (Simeonidis *et al.* 2007). The synthesis of metal structures by thermal decomposition of complexes is important because of easy control of purity, particle size and particles crystal structure (Niasari *et al.* 2009). Farhadi *et al.* (2013) prepared Co_3O_4 sphere-like nanoparticles with an average size of 19 nm by decomposing $Co(NH_3)_3(NO_2)_3$ complex at 175 °C. The decomposition of the complex was done by transferred the dry powder into a porcelain dish then heated. Peng *et al*. (2009) reported that this method usually requires high temperatures above 300 °C. The temperature varies depending on the metal complex. The reaction

temperature may go above the flammable point of the organic compounds (Jana *et al.* 2004). The synthesis of Co_3O_4 nanoparticles was very difficult when the reaction temperature was below 300 °C (Jana *et al*. 2004). The obtained particles were a mixture of shapes from cobalt stearate. Formation of Co_3O_4 nanoparticles was obtained with the temperature above 320 °C.

1.1.2.3 Hydrothermal method

Hydrothermal is defined as a heterogeneous reaction in the presence of solvents or mineralizers under high pressure and temperature conditions (Mohapatra & Anand 2010). The generated pressure from water upon heating enhances the solubility and the reactivity of the reactants can improve the crystallinity of the prepared nanocrystals (Sun *et al*. 2013). However, this method uses high pressures. The influence of synthesis routes was studied by Amiri *et al*. (2011). They conducted a hydrothermal method with post heat treatment. Their results showed that the synthesized Co_3O_4 nanoparticles were obtained after calcining β-$Co(OH)_2$ at different temperatures at 300, 600 and 900 °C for 2 hours. The increase in calcination temperature increases the crystallite sizes from 10 nm at 300 °C, 37 nm obtained at 600 °C and 57 nm at 900 °C. Pan *et al*. (2014) synthesized Co_3O_4 nanoparticles via a hydrothermal process of cobalt hydroxide precursor. The results showed that Co_3O_4 hexagonal nanodiscs were 20 nm in size. An additional step of heating of the precursor at 450 °C for 2 hours was done in order to obtain Co_3O_4 nanodiscs. Hydrothermal synthesis at low temperature and low pressure produces cobalt hydroxide instead of Co_3O_4, therefore in order to produce Co_3O_4 from the hydrothermal process, high temperatures and pressures are required (Amiri *et al*. 2011). The above-mentioned synthesis of Co_3O_4 showed that heat treatment should be applied in order to transform cobalt hydroxide into Co_3O_4 particles.

1.1.2.4 Chemical precipitation method

Chemical precipitation method is an easy technique and effective chemical method to achieve cobalt oxide and iron oxide nanoparticles (Mohapatra & Anand 2010). Advantages of this method include easy control; a lot of nanoparticles can be synthesized, low temperature and simple apparatus (Xie & Shen 2009). However, the control of particle size distribution is limited, because only kinetic factors are controlling the growth of the crystal. In the precipitation process, two stages are involved that is a short burst of nucleation occurs when the concentration of the species reaches critical supersaturation, and then, there is a slow growth of the nuclei by diffusion of the solutes to the surface of the crystal (Mohapatra & Anand 2010). The synthesis of Co_3O_4 nanocubes was achieved by Xu & Zeng (2003) using NaOH as the precipitating agent at 95° C. Uniform size of 47 nm were obtained by precipitating cobalt hydroxide and hydroxide nitrate. This method was chosen because it is cheap, has the ability to prevent agglomeration due to low solubility of the particles and control of particle size can be achieved.

1.1.2.5 Microwave irradiation method

Microwave irradiation has been given attention due to its unique reaction effects such as rapid heating and the increase in reaction rate. In comparison with other methods, microwave technique has the advantages such as short reaction time, small particle size, narrow particle size distribution, low energy budget and high purity (Vijayakumar *et al.* 2013). Different researchers have achieved Co_3O_4 nanoparticles via microwave-assisted route within a shorter space of time ranging from 5-20 minutes. The polarity of the solvent for this technique is

important. Water is considered as one of the best solvents to absorb microwaves and convert them into heat energy because it has a high dipole moment (Zhu *et al.* 2001).

Sun *et al*. (2011) have prepared Co_3O_4 nanoparticles using a temperature of 180 ºC for 20 minutes and a mixture of organic solvents and water was used. Cobalt oleate was used and the bond between the oxygen and carbon in the complex may have been thermally cleaved to form Co_3O_4. The method produced Co_3O_4 nanocubes of 20 nm after heating in the microwave. In another study, Shinde *et al*. (2015) reported the use of ethylene glycol and water as solvents at 270 Watts in the presence of cobalt acetate and sodium carbonate as precursors. Cobalt hydroxycarbonate-ethylene glycol complex was obtained. The obtained Co_3O_4 was spheres, rods, triangles and cubes rectangles with sizes ranging from 20-200 nm after calcination at 400 °C. Bhatt *et al.* (2011) used a microwave irradiation on a mixture of cobalt nitrate and ethylene glycol for 5 minutes. Co_3O_4 spheres ranging from 3-12 nm after heating at 40 °C for 3 h in the air were obtained. This method was chosen because it is easy and has the ability of producing nanoparticles within short time. This method also accelerates the reaction in an aqueous medium as compared conventional heating method.

1.1.3 The effect of capping molecules on the shape of nanoparticles

Capping molecules are substances that adsorb on the surface of the nanoparticles with the aim of preventing the reaction and the particle growth during the synthesis (Vadlapudi 2015). They have a vital role in controlling the size and shape of the nanoparticles (Xu & Zeng 2004). Capping molecules also offer the stability of the nanoparticles. Nucleation and growth process must be tuned in order to obtain shape control (Xiao & Qi 2011). There are two ways in which shape control can take place; it can either take place kinetically or thermodynamically (Xiao & Qi 2011). In the thermodynamic control, the effect of surface energy becomes important in determining the shape**.** The surface with the lowest surface energy will direct which shape is

obtained (Xiao & Qi 2011). The capping molecules which may result in changing the relative surface energy of different planes causing the shape to change because they adsorb with different strengths on surfaces with different miller indexes (Xiao & Qi 2011). Co_3O_4 nanocubes are formed under thermodynamic control whereby a low growth rate take place (Zhang *et al.* 2007). The nanocubes {100} planes are said to have low surface energy. These planes are associated with the cubic symmetry of Co_3O_4. Therefore the growth of Co_3O_4 gets terminated at these planes under thermodynamic conditions. As a result, the nanoparticles will have cubic morphology. Kinetic control deals with how fast a particular surface of the nanoparticles can grow leading to different particle shapes. Capping molecules can kinetically control the shape of the nanoparticles, by direct growth mechanism and oriented attachment (Xiao & Qi 2010). In the direct growth mechanism, the growth of the particles will be slower where the capping is strongly adsorbed. Growth takes place where the capping molecule is weakly adsorbed and therefore the growth will take place on these certain crystal surfaces. For the oriented mechanism, the particles will arrange themselves on the sites where the capping molecules are weakly adsorbed. Nanoparticles come together using these surfaces to form certain shapes. The growth will then prefer to take place in the direction where the capping molecules are weakly adsorbed. The length and the type of capping agents used can differ significantly and therefore impacting the size of the resulting nanoparticles.

1.1.4 Influence of length of capping molecules on shape and size of nanoparticles

The length of the capping molecule is vital into controlling the growth and shape of nanoparticles and therefore different shapes may be obtained when capping molecules with different lengths are used (Demortiere *et al.* 2008). Different alkyl chains of cetyltrimethyl ammonium bromide (CTAB) were used as a surfactant in the synthesis of gold nanorods by reduction of Au (III) to Au (0) (Gao *et al.* 2003). Different carbon chain lengths of CTAB (n= 10,12,14,16 and 18) were used. Surfactants used in the study by Gao *et al.* (2003) produced a mixture of spheres and nanorods**.** This means that the trimethylamine head group alone could not selectively form gold nanorods. The number of nanorods formed relative to nanospheres was increased when the alkyl chain length was increased. The higher aspect ratio of nanorods was obtained when the alkyl chain length was increased. Bilayers formed in a zipping mechanism via the tails of the hydrocarbon when long alkyl chain lengths were used. Formation of bilayers of the surfactants on the surface of the nanorods provided additional stabilization leading to nanorods formation. This showed that the length of the surfactants was important for producing gold nanorods.

When capping molecules are adsorbed onto the surface of the nanoparticles, the rate of their growth and thus size may be influenced (Mohapatra & Anand 2010). Demortiere *et al.* (2008) study showed that the length of the capping molecule is vital in reducing $PtCl_6^{2-}$ during the synthesis of platinum nanoparticles. Different alkylamines were used as capping agents to obtain cubic shaped nanoparticles of different sizes. Different alkylamine capping molecules, hexadecyl amine ($C_{16}H_{33}NH_2$), dodecyl amine ($C_{12}H_{25}NH_2$), and octylamine ($C_8H_{17}NH_2$), were used. The alkylamine with the longest hydrocarbon chain ($C_{16}H_{33}NH_2$) produced 2.3 nm, ($C_{12}H_{25}NH_2$) yielded 3.2 nm and $C_8H_{17}NH_2$ produced cubes of 5.5 nm. The nanoparticle size decreased with an increase in the chain length. The particles with the smallest size were due to

the lower solubility and higher steric hindrance of the longer chain capping agents in toluene. A decrease in the solubility of the capping molecule may have led to a stronger adsorption on the nanoparticle surface restricting access to the surface of the particles, therefore, slowing the rate of growth and decreasing the size.

Yin *et al*. (2004) studied the influence of different carboxylic acids using octanoic acid, lauric acid, and oleic acid with different alkyl chain lengths in the thermal decomposition of $[Fe(CO)_5]$**.** The size of the ɣ- Fe_2O_3 nanoparticles was 6 nm, 9 nm, and 12 nm when octanoic acid ($C_8H_{16}O_2$), lauric ($C_{12}H_{24}O_2$) acid and oleic acid ($C_{18}H_{34}O_2$) were used respectively. The size of ɣ-Fe_2O_3 nanoparticles increased as the chain of the carboxylic acid increased. The decomposition of the iron carbonyl also increased from 264 to 288 °C with an increase in the hydrocarbon chain length which implied that the nanoparticles capped with the oleic acid were prepared at a higher temperature than that of nanoparticles capped with octanoic acid and this may explain why the nanoparticle sizes increased with an increase in the capping molecule's length. The head-group of capping molecule used and the preparation method in the study by Yin *et al.* (2004) is different from the study by Demortiere *et al.* (2008) leading to different reasons for the change in the size of the nanoparticle with the length of the capping molecule. This may be the reasons why different relationships between the length of capping molecule and the size of the nanoparticles were found.

1.1.5 Influence of carboxylate ion on shape of the cobalt oxide nanoparticles

The carboxylate ion (COO^-) is the carboxyl group from the carboxylic acid (COOH). The carboxylates can provide coordination and prevent aggregation (Monfared *et al.* 2015). These carboxyl groups are used for the interaction in complexes and for metal oxides. Carboxylate group has a strong affinity to Co^{3+} and favors attachment of carboxylate on the surface of the particles (Monfared *et al.* 2015). Figure 2 shows the schematic of bonding modes of metal

carboxylate. Figure 2 (a) shows the chelating mode where the metal is centered between two oxygen atoms and attracted to both oxygen atoms. The bridging mode in Figure 2 (b) shows that each carboxylate oxygen atom is coordinated to one metal (Schneller & Griesche 2013).

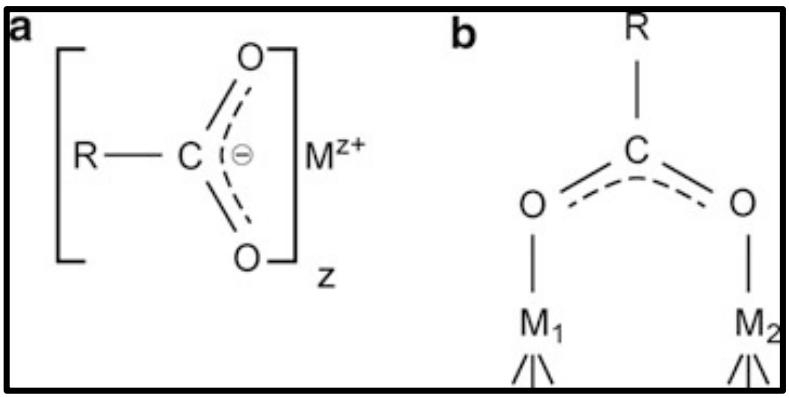

Figure 2: Scheme of different bonding modes of metal carboxylates. M, M_1, and M_2 represent the metal ion (where M_1 and M_2 can be different), z is the charge and R are the organic moieties consisting of carbons (Schneller & Griesche 2013).

Xu and Zeng (2004) used polyoxyethylene (20) sorbitan trioleate (TWEEN-85), as capping molecule which resulted in the formation of Co_3O_4 nanoparticles with cubic shapes of sizes between 3.5-5.7 nm. The results indicated that TWEEN-85 (an ester) was hydrolysed forming a carboxylate ion (oleate ion) which adsorbed onto the surface of Co_3O_4 nanoparticles. Yang *et al.* (2007) also formed Co_3O_4 nanoparticles with cubic morphology with an average size of 18 nm when cobalt acetate was used as a cobalt source instead of cobalt nitrate and cobalt sulfate. Based on the findings of Xu & Zeng (2004) and Yang *et al.* (2007), one may say that the carboxylate ion played an important role in the formation of cubic shaped Co_3O_4 nanoparticles. The length of the carboxylate ions used in these two studies differed significantly, therefore, a question could be raised if the length has an influence on the size of the resulting cobalt oxide

nanoparticles. Both studies used a precipitation-oxidation preparation method but different oxidizing agents were used.

1.1.6 Influence of pH on the size and shape of cobalt oxide nanoparticles

The pH of the solution during the synthesis of nanoparticles can be regulated by using sodium hydroxide, NaOH. The proper amount of NaOH can be used to control the pH and therefore produce particles that are uniform and having a narrow size distribution (Li *et al*. 2011). The size and shape of nanoparticles can be influenced by the amount of hydroxide ion (Shahmiri *et al*. 2013).

The effect of pH using NaOH was studied by Agnihotri *et al*. (2013) during the synthesis of silver, Ag nanoparticles. Three different ranges of pH were studied, namely 5-7, 8-11 and 12-13. The nanoparticles obtained in the pH range of 5-7 were irregular and large as compared to the pH range of 8-9. At the pH range of 10-11, the obtained shape was spherical and monodispersed. A further increase in pH (12-13) yielded nanorods. As the pH increases the size of the Ag nanoparticles decreased. Not only does the alkalinity of the solution influence size distribution but also the morphology. Li *et al*. (2011) synthesized gold nanoparticles in the presence of NaOH. The aim of their study was to use NaOH in order to decrease polydispersity. The results showed that as the NaOH concentration increases, the polydispersity decreases. The increase in NaOH concentration also played a role in the size distribution. An increase in NaOH produced uniform gold nanoparticles with a narrow size distribution.

Zinc acetate, $Zn(CH_3COOH)_2.2H_2O$ and NaOH were used to synthesize zinc oxide, ZnO nanoparticles (Ikono *et al*. 2012). To test the influence of pH, the size of the nanoparticles were measured at pH lower than 7, 8, 10 and 12. The results indicated that the nanoparticles were 10, 17, 38 and 74 nm respectively. As the pH increased the size of the nanoparticles also

increased. At pH 7 almost no ZnO nanoparticles were formed. For pH lower than 7 a mixture of compounds such as zinc hydroxide and sodium acetate was obtained. As the pH increased pure ZnO was obtained at pH 12. High purity ZnO nanoparticles obtained at high pH were due to the fact that ZnO tends to bind each other and agglomerate hence larger particle size was obtained (Ikono *et al*. 2012).

1.1.7 Influence of time on the size of cobalt oxide nanoparticles

One of the parameters which can be used to control the size of nanoparticles is time due to the fact that nucleation and growth are time dependent. Feng & Zeng (2003) varied the time during the synthesis of Co_3O_4 nanocubes in order to control the size. Their results showed that the nanoparticles prepared at 3 hours gave 11.2 nm, 6 hours produced 24.3 nm and when the reaction time is increased to 24 hours the obtained size is 44.7 nm. This indicated that the size of the nanoparticles increased as the aging time was increased. Synthesis of Co_3O_4 nanocubes was prepared by Liu *et al.* (2005) showed that the nanocubes synthesized from 4 hours ranged from 5-10 nm, for 8 hours the size obtained was 15 nm. The nanocubes prepared for 12 hours yielded particles which were 20 nm in size. Teng *et al*. (2010) prepared Co_3O_4 nanocubes by varying the aging time at 3, 6, 12 and 18 hours. The particles aged for 3 hours showed a mixture of $Co(OH)_2$ and Co_3O_4. As the time increases to 6 hours to 18 hours the amount of $Co(OH)_2$ decreased while Co_3O_4 increased. Teng *et al*. (2010) study showed that a mixture of products was obtained due to the absence oxidizing agent**.** The growth process of Co_3O_4 nanoparticles was investigated by Kang & Zhou (2015).The reaction time was varied from 2, 9, 18, 27 and 36 hours in order to investigate the growth process of the nanoparticles. Irregular shapes were obtained at the reaction time of 2 hours. Cube-like particles with a wide size distribution were obtained at a reaction time of 9 hours. As the time increased from 18, 27 and 36 hours irregular

cube-like particles became less and more uniform cubes were observed. The above-discussed literature shows that the longer the reaction process, the desired products can be obtained.

1.1.8 Effect of precursor on the shape cobalt oxide nanoparticles

The effect of precursors has been studied by Yang *et al*. (2007) on the morphology of Co_3O_4 nanoparticles using cobalt salts. Uniform shape-controlled Co_3O_4 nanoparticles were investigated by using different cobalt sources namely, cobalt nitrate, cobalt acetate and cobalt sulphate. Irregular morphologies were obtained when cobalt nitrate was used, cubic morphology from cobalt acetate and spherical shape from cobalt sulphate. Kim & Park (2012) prepared Co_3O_4 nanoparticles of different morphologies. Their results showed that cube type Co_3O_4 particles were obtained using cobalt nitrate and flower type when cobalt chloride was used. Cobalt chloride, cobalt nitrate, cobalt acetate and cobalt sulfate were used as cobalt precursors by Hussain *et al*. (2014). The study of chloride anion effect on the shape of Co_3O_4 nanostructures obtained nanowires. Nitrate anion changed the shape of Co_3O_4 into honey comb like porous nanomaterials. The study of acetate anion showed Co_3O_4 grass-like shape composed of thin wires. The fourth cobalt source from the sulfate gave nanosheets like shape morphology. From the above literature, it shows that the anion type in cobalt salt plays an important role in the morphology of Co_3O_4 nanoparticles.

1.1.9 Influence of the oxidant on the synthesis of cobalt oxide nanoparticles

Oxidizing agents are important during the synthesis of cobalt oxide nanoparticles. This is because, Co^{2+} in cobalt hydroxide, $Co(OH)_2$ must be oxidized to Co^{3+} in Co_3O_4 Teng (2010) and the amount of oxidant should be sufficient in order to obtain Co_3O_4 with spinel crystal structure (Yang *et al.* 2007). Amiri *et al.* (2011) studied the use of oxidant using hydrogen peroxide, H_2O_2 in the synthesis Co_3O_4 nanoparticles. The results showed that the side effect of the post heat treatment of synthesized cobalt oxide was eliminated. However, the production of Co_3O_4 in the H_2O_2 assisted method was highly dependent on the amount of H_2O_2. If an inadequate amount of H_2O_2 was added to the synthesis process, the resulting structure was composed of β-$Co(OH)_2$ and Co_3O_4. With higher amounts of H_2O_2, the structure was pure Co_3O_4. The increase in the amount of hydrogen peroxide reduced the presence of cobalt hydroxide and hence more cobalt oxide was formed. Not only does H_2O_2 have an influence on the type of product formed but also on the size of cobalt oxide nanoparticles. Using hydrogen peroxide as compared to oxygen may change the rate of the reaction. This is because H_2O_2 is a stronger oxidizing agent as compared to oxygen. This is shown by the reduction potentials energy values from the half reactions of oxygen and hydrogen peroxide. The reactions are given below (MacMurry *et al*. 2012):

$H_2O_2\ (aq) + 2H^+(aq) + 2e^- \longrightarrow 2H_2O\ (l)$ 1.78 V Equation 1

$O_2\ (g) + 4H^+\ (aq) + 4e^- \longrightarrow 2H_2O\ (l)$ 1.23 V Equation 2

The change in the reaction rate will have an influence on the size of nanoparticles. Jiang *et al.* (2002) have obtained cobalt oxide nanoparticles ranging from 3-4 nm. Neltner *et al.* (2009) have also synthesized cobalt oxide using H_2O_2 and they have obtained nanoparticles which were very small with sizes of 1 nm or less. The use of H_2O_2 has also shown an advantage of

preventing particle growth and hence the formation of smaller sizes (Neltner *et al*. 2009). Oxygen is also as an oxidant which is used during the synthesis of Co_3O_4 nanoparticles. The synthesis of Co_3O_4 nanocubes was obtained by Feng & Zeng (2003) using precipitation method and oxygen as an oxidant. Their study showed spinel cobalt oxide nanocubes was obtained with the edge length ranging from 10-100 nm. Dong *et al*. (2007) obtained Co_3O_4 particles 70 nm in size when oxygen was used as an oxidant.

1.1.10 Factors affecting the reaction rate of cobalt oxide nanoparticles

The reaction rate is defined as the increase in the concentration of the product per unit time or as the decrease in the concentration of the reactant per unit time (MacMurry *et al*. 2012). Factors that affect the rate of a reaction include temperature and concentration (MacMurry *et al*. 2012). For many reactions, the reaction rate will increase as the concentration of the reactants increases. The more the particles collide per unit time, the more the reaction between will occur. Therefore, the rate will increase as the concentration increases. Usually, when the concentration of a reactant doubles the reaction rate will also double. Increasing the temperature of the system increases the average kinetic energy of the particles. As the kinetic energy increases the particles move faster and more collision occurs. Both these factors increase the rate of the reaction. Hence the increase in temperature increases the reaction rate. The ionic strength of the solution can also increase the rate of the reaction.

Xu & Zeng (2003) have formed cobalt oxide nanocubes by varying the concentration of sodium nitrate, $NaNO_3$ as a precursor. In their study, it shows that sodium nitrate played a key role in changing the structure and the chemical composition of the precursor which lead to different reaction paths and reaction rate to get cobalt oxide nanoparticles. The increase in sodium nitrate amount has led to an increase in the ionic strength of the reaction which ultimately increased

the reaction rate (Xu & Zeng (2003). This also plays an important role in controlling the size and the shape Co_3O_4 nanoparticles.

1.2 Problem statement

Phenol is often used as a model compound for wastewater treatment studies. Phenols and their derivatives are considered as major hazardous compounds that are found in industrial wastewater and can cause major environmental damage if not treated (Aljoubory & Senthilkumar 2014). It is the priority pollutant since it is toxic and harmful to organisms even at low concentrations (Das *et al.* 2014). Surface and ground waters are contaminated by phenolics as a result of the continuous release of these compounds from petrochemical, coal conversion and phenol producing industries. Therefore, wastewaters containing phenolic compounds must be treated before their discharging into the water streams. Cobalt oxide nanoparticles are believed to catalyze the decomposition of phenol by ozone (Dong *et al*. 2010) compared with bulk cobalt oxide. The shape of a nanocrystallite may influence the properties of the crystallite (Xia *et al*. 2014). Therefore, it is of interest to prepare cobalt oxide crystallites of different morphologies and sizes that will be used as catalysts because the challenges in synthesizing nanoparticles are not only about the shape but also about the size (Niasari *et al.* 2009).

1.3 Motivation

Cobalt oxide has received a lot of attention because it is an effective heterogeneous catalyst for use in solid-state sensors (Teng *et al*. 2010). The catalytic activity of the catalyst depends on the shape and the size of the crystal. It is therefore interesting to synthesize cobalt oxide nanoparticles of different sizes and shapes that can be used as a catalyst in future studies. The synthesis of nanoparticles sometimes requires the addition of capping molecules. Capping molecules are also referred to as adsorbates or surfactants. Surface-capping agents are used for stabilizing the surface of nanoparticles by preventing the further growth and they can also change the morphology, optical properties and structure of nanoparticles (Rahdar 2013). Organic materials such as carboxylic acids are used during the synthesis of metal oxide as capping molecules. In this study, the choice of capping molecule is acetic acid (CH_3COOH). In carboxylic acids, the acid is believed to react with the metal around the surface of the nanoparticles and get adsorbed on the surface by chemisorption (Thomas *et al*. 2009). The carboxyl group from the carboxylic acid provides coordination to the nanoparticles and stabilization (Monfared *et al*. 2014).

1.4 Aim and Objectives

The aim of this research was to study the effect of carboxylic acids on size and shape of cobalt oxide nanoparticles. The following objectives were set out for this study:

a) Synthesis cobalt oxide nanoparticles through the microwave technique by decomposition of the cobalt carboxylate complexes.
b) Synthesis of cobalt oxide nanoparticles using chemical precipitation with oxidation method.
c) Investigation of various parameters of synthesis including the time, oxidant, NaOH concentration, and acetate content.
d) Characterization of synthesized nanoparticles.

The prepared complexes and cobalt oxide nanoparticles were characterized by a combination of spectroscopic techniques (UV-vis, PL, and FTIR), XRD, TEM, TGA, Elemental Analyses and particle size analysis techniques.

References

AGILANDESWARI K & KUMAR, A.R. 2014. Synthesis, characterization and optical properties of Co_3O_4 by precipitation method. *International Journal of ChemTech Research*, 6, 2089-2092.

AGNIHOTRI, S., MUKHERJIA, S. & MUKHERJIA, S. 2014. Size-controlled silver nanoparticles synthesized over the range 5-100 nm using the same protocol and their antibacterial efficacy. *RSC Adv*ances 4, 3974-3983.

ALJOUBORY, D., A. & SENTHILKUMAR, R. 2014. Phenol degradation of industrial wastewater by photocatalysis. *Journal of Innovative Engineering*, 2, 1-5.

ANDAL, V & BUVANESWARI. 2017. Effect of reducing agents in the conversion of Cu_2O nanocolloid to Cu nanocolloid. *Engineering Science and Technology, an International Journal,* 20, 340-344.

AMIRI, S.E.H., VAEZI, M.R., & KANDJANI A.E. 2011. A comparison between hydrothermally prepared Co_3O_4 via H_2O_2 assisted and calcination methods. *Journal of Ceramic Processing Research*, 12, 327-331.

BA-ABBAD, M.M., KADHUM, A.A.H., MOHAMAD, A.B., TAKRIFF, M.S. & SOPIAN, K. 2012. Synthesis and catalytic activity of TiO_2 nanoparticles for photochemical oxidation of concentrated chlorophenols under direct solar radiation. *International Journal Electrochemical Sci*ence 7, 4871- 4888.

BABU, G. A., RAVI, G. & HAYAKAWA, Y. 2015. Microwave synthesis and effect of CTAB on ferromagnetic properties of NiO, Co_3O_4 and $NiCo_2O_4$ nanostructures. *Journal of Applied. Physics. A*, 119, 219-232.

BHATT, A.S.,BHAT, D.K.,TAI,C & SANTOSH, M.S. 2011. Microwave-assisted synthesis and magnetic studies of cobalt oxide nanoparticles. *Materials Chemistry and Physics,* 125, 347-350.

BEZEMER, G.L., BITTER J.H. & KUIPERS, H.P.C.E. 2006. Cobalt particles size effects in the Fischer-Tropsch reaction studied with carbon nanofibre supported catalysts. *Journal of Catalysis,* 1-3, 291-302.

CHEN, Y., ZHOU, J., MAGUIRE, P., O'CONNELL, R., SCHMITT, W., LI, Y., YAN, Z., ZHANG, Y., & ZHANG, H. 2016. Enhancing capacitance behaviour of CoOOH nanostructures using transition metal dopants by ambient oxidation. *Scientific Reports*, 6, 1-7.

DAS, B.C., SINHA, P. SUBHASISH, K.M., BANIK, D., DAS. M. 2014. Studies on removal of Phenol from contaminated water source by microbial route using Bacillus cereus. *International Journal of Current Research and Academic Review*, 2, 179-184.

DEMORTIERE, A., LAUNOIS, P., GOUBET, N., ALBOUY, P.A. & PETIT, C. 2008. Shape-controlled platinum nanocubes and their assembly into two-dimensional and three-dimensional superlattices. *Journal of Physical Chemistry,* 112*,* 14583-14592.

DONG, Y., HE, K., YIN, L. & ZHANG, A. 2007. A facile route to controlled synthesis of Co_3O_4 nanoparticles and their environmental catalytic properties. *Nanotechnology*, 18, 1-6.

DONG, Y., WANG, G., JIANG, P., ZHANG, A., LIN YUE, L. & ZHANG, X. 2010. Catalytic ozonation of phenol in aqueous solution by Co_3O_4 nanoparticles. *Bulletin of the Korean Chemical Society*, 31, 2830-2834.

ELHAGA, S., IBUPOTOA, Z.H., LIUB, X., NURA, O. & WILLANDER, M., 2014. Dopamine wide range detection sensor based on modified Co_3O_4 nanowires electrode. *Sensors and Actuators B*, 203, 543-549.

FARHADI, S., SEPAHDAR, A. & JAHANARA, K. 2013. Spinel-type cobalt oxide (Co_3O_4) nanoparticles from the mer-$Co(NH_3)_3(NO_2)_3$ complex: preparation, characterization, and study of optical and magnetic properties. *Journal of Nanostructures*, 3, 199-207.

FENG, J. & ZENG, C., H. 2003. Size-controlled growth of Co_3O_4 nanocubes. *Chemistry of Materials*, 15, 2829-2835.

FENG, C., WANG, H., ZHANG, J., HU, W., ZOU, Z. & YIDA DENG, Y. 2014. One-pot facile synthesis of cobalt oxide nanocubes and their magnetic properties. *Journal of Nanoparicle Research*, 16, 2413.

FISCHER, N., VAN STEEN, E. & CLAEYS, M. 2011. Preparation of supported nano-sized cobalt oxide and fcc cobalt crystallites. *Catalysis Today*, 171, 174-179.

GAO, J., BENDER, C.M. & MURPHY, C. J. 2003. Dependence of the gold nanorod aspect ratio on the nature of the directing surfactant in aqueous solution. *Langmuir*, 19, 9065-9070.

HOU, Y., LI, J., WEN, Z., CUI, S., YUAN, C. & CHEN, J., 2014. Co_3O_4 nanoparticles embedded in nitrogen-doped porous carbon dodecahedrons with enhanced electrochemical properties for lithium storage and water splitting. *Nano Energy*, 12, 1-3.

HUSSAIN, M., IBUPOTO, Z. H., ABBASI, M. NUR, O. & WILLANDER, M. 2014. Effect of anions on the morphology of Co_3O_4 nanostructures grown by hydrothermal method and their pH sensing application, *Journal of Electroanalytical Chemistry*, 717, 78-82.

HU, L., SUN, K., PENG, Q., XU, B. & LI, Y. 2010. Surface Active Sites on Co_3O_4 nanobelt and nanocube model catalysts for CO oxidation. Journal of *Nano. Research*, 3, 363-368.

IKONO, R. AKWALIA, P., R. SISWANTO, BAMBANG W, SUKARTO, A. & ROCHMAN.N., T. 2012. Effect of pH variation on particle size and purity of nano Zinc oxide synthesized by sol-gel method. *International Journal of Engineering & Technology*, 12, 1-5.

JANA, N.R., CHEN, Y. & PENG, X. 2004. Size-and shape-controlled magnetic (Cr, Mn, Fe, Co, Ni), oxide nanocrystals via a simple and general approach, *Chemical Matter*, 16, 3931-3935.

JIN, L., WANG., J. QIAN, X., XIA, D. & DONG, M. 2015. Catalytic activity of Co_3O_4 nanomaterials with different morphologies for the thermal decomposition of ammonium perchlorate. *Journal of Nanomaterials*, 2015, 1-7.

KANG, M. & ZHOU, H. 2015. Facile synthesis and structural characterization of Co_3O_4 nanocubes. *AIMS Materials Science*, 2, 16-27.

KIM, K.S. & PARK, Y.J. 2012. Catalytic properties of Co_3O_4 nanoparticles for rechargeable Li/air batteries. *Nanoscale Research Letters.* 7, 1-6.

LEE, H., KIM, C., YANG, S., HAN, J.W. & KIM, J. 2011. Shape-controlled nanocrystals for catalytic applications. *Catalysis Surveys from Asia*, 16, 1-14.

LI, C., LI, D., WAN,G., XU, J. & HOU, W. 2011. Facile synthesis of concentrated gold nanoparticles with low size-distribution in water: temperature and pH controls. *Nanoscale Research Letters.* 6, 1-10.

LIU, X., QIU, G. & LI, X. 2005. Shape-controlled synthesis and properties of uniform spinel cobalt oxide nanocubes, *Nanotechnology*, 16, 3035-3040.

MALIK, M.A., WANI, M.Y., & HASHIM, M.A. 2012. Microemulsion method: A novel route to synthesize organic and inorganic nanomaterials. *Arabian Journal of Chemistry,* 5, 397-417.

MANIGANDAN, R., GIRIBABU, K., SURESH, R., VIJAYALAKSHMI, L., STEPHEN, A. & NARAYANAN, V. 2013. Cobalt Oxide Nanoparticles: Characterization and its electrocatalytic activity towards nitrobenzene. *Chemical Science Transaction,* 2, S47-S50.

McMURRY, R., C. FAY, C. & FANTINI, J. 2012. Chemistry sixth edition. Pearson Education Inc. A-18.

MASCOLO, M. C., PEI, Y. & RING, T.A. 2013. Room Temperature co-precipitation synthesis of magnetite nanoparticles in a large pH window with different bases. *Materials,* 6, 5549-5567.

MOHAPATRA, M & ANAND. S. 2010 Synthesis and applications of nano-structured iron oxides/hydroxides. A review. *International Journal of Engineering, Science and Technology,* 2, 127-146.

MONFARED, H., PARCHEGANI, F. & ALAVI, S. 2015.Carboxylic acid effects on the size and catalytic activity of magnetite nanoparticles. *Journal of Colloid and Interface Science,* 437, 1-9.

NIASARI, M.D., MIR, N. & DAVAR, F. 2009. Synthesis and characterization of Co_3O_4 nanorods by thermal decomposition of cobalt oxalate. *Journal of Physics and Chemistry of Solids,* 70, 847-852.

OZKAYA, T., BAYKAL, A., TOPRAK, M.S., KOSEOGLU, Y. & DURMUS, Z. 2009. Reflux synthesis of Co_3O_4 nanoparticles and its magnetic characterization. *Journal of Magnetism and Magnetic Materials,* 321, 2145-2149.

PAL, J. & CHAUHAN, P. 2010. Study of physical properties of cobalt oxide Co_3O_4 nanocrystals. *Material Characterization,* 61, 575-579.

PAN, A., WANG,Y., XUB, W., NIE, Z., LIANG, S., NIE, Z., WANG,C., CAO,G. & ZHANG, J. 2014. High-performance anode based on porous Co_3O_4 nanodiscs. *Journal of Power Sources*, 255, 125-129.

PENG, X., CHEN, Y., JANA, N. & SWANG, N. 2009. Synthesis control of metal oxide nanocrystal sizes and shape. Patent number: US 7, 531, 149 B2. 1-21.

PIUMETTI, M., FREYRIA, F.S. & BONELLI, B. 2013. Catalytically active sites and their complexity, a micro-review. *Journal of Fine Chemicals, Applied Chemistry and Biotechnology,* 13, 55-58.

RAHDAR, A. 2013. Study of different capping agents effect on the structural and optical properties of Mn-doped ZnS nanostructures. *World Applied Programming*, 3, 56-60.

SARFRAZ, A.K & HASANAIN, S.K. 2013. Size dependence of magnetic and optical properties of Co_3O_4 nanoparticles. *Acta Physical Polonica A*, 125, 131-144.

SCHNELLER, T., WASER, R., KOSEC, M. & PAYNE, D. 2013. Chemical solution deposition of functional oxide thin films, *Springer*, 1, 29-49.

SHAHMIRI, M., IBRAHIM, N. A., ZAINUDDIN, N., ASIM, N., BAKHTYAR, B., ZAHARIM, A. & SOPIAN. K. 2013. Effect of pH on the Synthesis of CuO nanosheets by quick precipitation method. WSEAS transactions on environment and development, 9, 137-146.

SHINDE, M., QURESHI, N., RANE, S., UTTAM MULIK, U & AMALNERKAR, D. 2015. Synthesis of cobalt oxide nanostructures by microwave assisted solvothermal technique using binary solvent system. *Physical Chemistry Communications*, 2, 1-9.

SIMEONIDIS, K., MOURDIKOUDIS, S., MOULLA, M., TSIAOUSSIS, I. & MARTINEZ-BOUBETA, C. 2007. Controlled synthesis and phase characterization of Fe-based nanoparticles obtained by thermal decomposition. *Journal of Magnetism and Magnetic Materials*, 316, 1-4.

SOLTANI, N., SAION, E., HUSSEIN, M. Z., BAHRAMI, A., NAGHAVI, K. & YUNUS, R. 2012. Microwave irradiation effects on hydrothermal and polyol synthesis of ZnS nanoparticles. *Chalcogenide Letters*, 6, 265-274.

SONG, X. C., WANG, X., ZHENG, Y., F. MA, R. & YIN, H. 2011. Synthesis and electrocatalytic activities of Co_3O_4 nanocubes. *Journal of Nanoparticle Research*, 13, 1319-1324.

SONG, H., KIM, F., CONNOR, S., SOMORJAI, G. A. & YANG. P. 2005. Pt nanocrystals: shape control and Langmuir-Blodgett monolayer formation. *Journal of Physical Chemistry B*, 109, 188-193.

SUN, C., SU, X. XIAO, F. NIU, C. & WANG, J. 2011. Synthesis of nearly monodisperse Co_3O_4 nanocubes via a microwave-assisted solvothermal process and their gas sensing properties. *Sensors and Actuators B*, 157, 681-685.

SUN, H., HA, M., TADE, M. O. & WANG, S. 2013. Co_3O_4 nanocrystals with predominantly exposed facets: Synthesis, environmental and energy applications. *Journal of Materials, Chemistry* A, 1, 14427-14442.

TANG, C-W., WANG, C-B. & CHIEN, S-H. 2008. Characterization of cobalt oxides studied by FT-IR, Raman, TPR and TG-MS. *Thermochimica Acta,* 473, 68-73.

TENG, Y., YAMAMOTO, S., KUSANO, Y., AZUMA, M. & SHIMAKAWA, Y. 2010. One-pot hydrothermal synthesis of uniformly cubic Co_3O_4 nanocrystals. *Materials Letters*, 64, 239-242.

THOMAS, L.A., DEKKER, L., KALLUMADIL, M., SOUTHERN, P., WILSON, M., NAIR, S.P., PANKHURST, Q.A. & PARKIN, I.P. 2009. Carboxylic acid-stabilized iron oxide nanoparticles for use in magnetic hyperthermia. *Journal of Materials Chemistry*, 19, 6529-6535.

XIA, S., YUA, M., HU, J., FENG, J., CHEN, J., SHI, M. & WENG, X. 2014. A model of interface-related enhancement based on the contrast between Co_3O_4 sphere and cube for electrochemical detection of hydrogen peroxide. *Electrochemistry Communications*, 40, 67-70.

XIAO, J. & QI, L. 2010. Surfactant-assisted, shape-controlled synthesis of gold nanocrystals. Nanoscale. *Journal of Royal Society of Chemistry*, 3, 1383-1393.

XIE, X. & WENJIE SHEN, W. 2009. Morphology control of cobalt oxide nanocrystals for promoting their catalytic performance. *The Royal Society of Chemistry Nanoscale,* 1, 50-60.

XIE, X., LI, X., LIU, Z., HARUTA, M. & SHEN, W. 2009. Low-temperature oxidation of CO catalyzed by Co_3O_4 nanorods. *Letter. Nature,* 45, 746-749.

XU, R. & ZENG, H. C. 2004. Self-generation of tiered surfactants superstructures for one-pot synthesis of CoO nanocubes and their close and non-close-packed organization. *Langmuir,* 20, 9780-9790.

XU, R. & ZENG, H. C. 2003. Mechanistic investigation on salt-mediated formation of free-standing Co_3O_4 nanocubes at 95 °C. *Journal of Physical Chemistry B, 107,* 926-930.

VIJAYAKUMAR,S., PONNALAGI, A.K., NAGAMUTHU, S. & MURALIDHARAN,G. 2013. Microwave assisted synthesis of Co_3O_4 nanoparticles for high-performance *Supercapacitors Electrochimica Acta*, 106, 500-505.

YANG, Y-P., HUANG, K-L., LIU, R-S., WANG, L-P., ZENG, W-W. & ZHANG, P-M. 2007. Shape-controlled synthesis of nanocubic Co_3O_4 by hydrothermal oxidation method. *Transactions of Nonferrous Metals Society of China*, 17, 1082-1086.

YANG, Y-P., LIU, R-S., HUANG, K-L., WANG, L-P., LIU, S-Q. & ZENG, W-W. 2007. Preparation and electrochemical performance of nanosized Co_3O_4 via hydrothermal method, *Transactions of Nonferrous Metals Society of China,* 17, 1334-1338.

YIN, M., WILLLIS, A., REDL, F., TURRO, N. J. & BRIEN, S. P. 2004. Influence of capping groups on the synthesis of ɣ-Fe_2O_3 nanoparticles. *Journal Materials Research,* 19, 1208-1214.

ZHANG, Y., LIUA, Y., FUA, S., GUOA, F. & QIAN, Y. 2007. Morphology-controlled synthesis of Co_3O_4 crystals by soft chemical method. *Materials Chemistry and Physics*, 104, 166-171.

ZHU,J., ZHOU,M., XU,J. & LIAO.X 2001. Preparation of CdS and ZnS nanoparticles using microwave irradiation. *Materials Letters,* 47, 25-29.

CHAPTER 2: METHODOLOGY

2.1 Chemicals and equipments

2.1.1 Chemicals

The following chemicals have been used in this study without any further purification. Hydrogen peroxide 30% (Labchem), sodium hydroxide (associated chemical enterprise), cobalt nitrate (Fluka Chemicals), 1-butanol 99.8%, (laboratory consumables and chemicals), hydrochloric acid 32% (laboratory consumables & chemicals), methanol > 99.8% (Sigma-Aldrich), cobalt acetate tetrahydrate (Sigma-Aldrich), acetic acid 98% (Promark Chemicals), ethanol 99% (Glassworld), stearic acid (Hopkin & Williams Ltd), cobalt carbonate hydrate (Sigma-Aldrich), heptanoic acid > 99% (Sigma-Aldrich), n-hexane 85% (Labchem), 1-octadecene 90% (Sigma-Aldrich), and were all analytical grades.

2.1.2 Characterization Equipments

Several techniques were used to characterize the complexes and cobalt oxide nanoparticles as described below.

2.1.2.1 Fourier-Transform Infrared spectroscopy

Fourier transform infrared (FTIR) spectra were measured using Perkin-Elmer 400 FT-IR/FT-NIR Spectrometer, universal attenuated total reflection (ATR) with the diamond detector at a wavelength from 650 cm^{-1} to 4000 cm^{-1}. There was no sample preparation for this method. The nanoparticles were loaded on the sample plate for analysis and measured directly. FTIR spectroscopy is usually used in the identification of functional groups found in organic

compounds and polymers. In this project, the technique was used to confirm the structure of the complexes and to determine the capping molecules that are adsorbed on the nanoparticles.

2.1.2.2 Thermogravimetric analysis

Thermogravimetric Analyser (TGA) used was a Perkin Elmer, simultaneous Thermal Analyser STA 6000 with scan temperature from 30 °C to 900 °C. Temperature ramp rate was 10° per minute with nitrogen gas flow of 20 ml min^{-1}, using nitrogen as an inert gas. The sample was loaded for analyses inside the sample holder. The change in sample weight was measured while the sample was heated at a constant rate (or at constant temperature). This technique is effective for quantitative analysis of thermal reactions of materials that are accompanied by mass changes, such as evaporation, decomposition, gas absorption, desorption and dehydration (Rajarathnam 2014).

2.1.2.3 Ultraviolet-visible spectroscopy

UV-vis analyses were performed with a double beam spectrometer - Perkin Elmer Lambda 25 UV/vis which collects spectra from 180-1100 nm UV and visible range using a bandwidth of 1 nm with a fixed slit. Tungsten and deuterium lamps were used for illumination. A baseline setting was done by using water as a reference sample. A very small amount of the solid sample/crystals was dissolved in water. This solution was scanned and measured. The baseline correction was done automatically by the instrument by subtracting it from the measured results. The optical band gap determination is done by investigating the dimensional and shape effects on the energy absorption. The band gap energy was calculated using the wavelength at peak maximum for each absorption peak.

2.1.2.4 Photoluminescence spectroscopy

The emission of the nanoparticles was determined using Jasco Spectrofluorimeter FP-8600 equipped with XE lamp, 150 W. The bandwidth excitation slit at 5 nm and the emission ranging from 200-1010 nm. Fluorescent materials absorb UV light and emit light of longer (frequency visible) wavelength. The instrument consists of a UV source; a monochromator for selection of the desired wavelength for irradiation, a sample holder, a second monochromatic is used to select the desired wavelength of detection and a phototube amplifier-output assembly. The fluorometer irradiates then records the intensity of the light emitted by the sample on a plate. Photoluminescence (PL) were used to determine the optical properties of the nanoparticles.

2.1.2.5 Carbon, hydrogen, nitrogen and sulfur analysis

The determination of the elemental composition of samples was conducted using Flash 2000 CHNS-O analyzer fitted with auto-sampler. The sample was combusted in an oxygen environment using 250 kPa. The analyzer uses the combustion process to break down substances into simple elements which are then measured. The masses of these combustion products are used to calculate the composition of the unknown sample. The determination of carbon and hydrogen percentage was done through this technique. Therefore the reconstruction of the organic molecule adsorbed onto the surface of the nanoparticles can be evaluated.

2.1.2.6 Transmission electron microscopy

The size and shape of the nanoparticles were determined using an LEO TEM 912 with an acceleration voltage of 120 kV and a tungsten wire filament. The fine nanoparticles dispersed in the methanol were pipetted out and placed on activated carbon-coated copper grids. This was allowed to dry then placed on transmission electron microscopy (TEM) sample holder and loaded on in the instrument. Images were taken with a Proscan slow scan CCC digital camera

to establish the crystal size and the distribution of nanoparticles. An average of 100 particles was measured using the ImageJ software from the images for each sample.

2.1.2.7 X-ray diffraction

A Bruker D2 (D2-205530) diffractometer using secondary graphite monochromated CuKα radiation (λ=1.78897Å) at 30 kV/30 mA was used to measure x-ray diffraction (XRD) patterns of the as-prepared samples. Measurements were taken using a glancing angle of incidence detector at an angle of 2°, for 2θ values over 20 - 110° in steps of 0.026° with a step time of 37s and at a temperature of 294 K. The raw data file was converted to an Excel readable file using the software PowDLL Converter. The FWHM (Full-Width at Half-Maximum) was determined to fit a Gaussian peak using the Fityk software program. The determined FWHM was used to calculate the crystallite size through Debye-Scherrer equation:

$$D = K\lambda/\beta cos\,\theta$$

K is the Scherrer constant for spherical shape, typically set as equal to 0.9, λ represents the X-ray wavelength used for the measurement, β is the line length of FWHM, determined in 2θ (θ is the Bragg angle), and D is the crystalline size (nm).

2.2 Preparation of the cobalt complexes

The preparation of cobalt complexes was adopted from Ley (2009). Cobalt complexes, cobalt acetate, cobalt heptanoate and cobalt stearate were prepared from carboxylic acids, namely: acetic acid, heptanoic acid, and stearic acid as ligands. A mass of 11.90 g cobalt (II) carbonate hydrate was dissolved in 50 mL hot (61 °C) de-ionized water. A volume of 12 mL acetic acid was added dropwise with a dropper into the cobalt carbonate solution. Thereafter the reaction temperature was heated to 100 °C until the volume of solvent was reduced to approximately 20 mL. The mixture was allowed to cool to room temperature and stand for 24 hours. A formation of a wax was observed. This was washed with cold 200 mL of n-hexane. After four days the wax changed to crystals which were dried at 90 °C for 4 hours. The above procedure which describes the preparation of cobalt acetate was also used to prepare cobalt heptanoate and cobalt stearate. The masses used were: 11.89 g cobalt (II) carbonate hydrate and 26 mL heptanoic acid, 11.88 g cobalt (II) carbonate hydrate and 56.89 g stearic acid. The percentage yield were 16.7, 89.60 and 93.15% for cobalt acetate, cobalt heptanoate and cobalt stearate.

2.3 Synthesis of cobalt oxide nanoparticles from cobalt complexes using the microwave irradiation technique

The preparation of cobalt complexes was adopted from Sun *et a*l. (2011). A solvent of 30 mL of 1-octadene was added into 1.25 g of cobalt acetate (commercial) in a beaker. The solution was heated by using hot water then applied ultra-sonication for 20 minutes to dissolve the complex and to have a homogenous sample. Ethanol (15 mL) was used as the solvent. The same type of nanoparticles was synthesized using 1.86 g cobalt heptanoate and 3.11 g cobalt stearate. The samples were poured into a Teflon microwave sample holder and then placed into

a microwave digester. The reactions were heated to 200 °C for 12 minutes. After the reaction had completed the samples were cleaned with 50 mL of n-hexane 3 times followed by 50 mL of ethanol twice and then 3 times with 2M HCl. The last cleaning was done with deionized water. Cobalt stearate and cobalt heptanoate were washed with 1-octadecene and then dried in the fume hood. Cleaning was conducted through centrifugation at 5000 rpm for 5 minutes.

2.4 Preparation of cobalt oxide nanoparticles from chemical precipitation with oxidation method using oxygen

Chemical precipitation method was adopted from Xu & Zeng (2004). A concentration of 0.2 M of sodium hydroxide was dissolved in 100 mL deionized water in a three-necked round bottom flask while stirring. Cobalt acetate solution prepared from the dissolution of 4.99 g in 10 mL of deionized water was added to the sodium solution. The pH of 7.91 was recorded at room temperature. The flask was connected to a condenser and heated between 80-85 °C. The reaction mixture was then bubbled with air at 143 mL per minute for 72 hours using a 10-20 µm ace gas dispersion tube with a porous fritted glass tip. The air was supplied by an aquarium air pump. After the reaction, the flask was cooled in a water bath then 50 mL of ethanol was used to flocculate the nanoparticles. This was performed 3 times using a centrifuge for 5 minutes at 5000 rpm. Thereafter 2 M of 50 mL hydrochloric acid was used 3 times to clean the precipitate. The product was cleaned twice with 50 ml deionized water. Methanol was used for final removal of water. Once the washing was completed, the nanoparticles were air dried in the fume hood for 3 days, followed by characterization. The same type of nanoparticles was synthesized and their compositions were: 0.3 M of sodium hydroxide and 4.99 g of the cobalt acetate. The pH of the mixture was recorded as 8.49. On the other hand, the same type of particles was prepared using 0.4 M of sodium hydroxide, 4.98 g of cobalt acetate. The pH of

10.18 was recorded. The last composition was 0.7 M sodium hydroxide with 4.98 g of cobalt acetate with pH of 12.26. The effect of acetate was studied by using cobalt nitrate in order to compare the nanoparticles prepared from cobalt acetate. The amount used for cobalt nitrate was: 0.3 M of sodium hydroxide and cobalt nitrate with a mass of 5.88 g. The pH of the mixture was recorded as 8.77.

To study the effect of time, the same types of nanoparticles were prepared over 16 hours, 44 hours and 72 hours as adopted from Xu & Zeng (2004), Yang *et al*. (2007) using 0.4 M sodium hydroxide. The compositions used for 16 hours were: 0.4 M of sodium hydroxide, 4.99 g of cobalt acetate. The pH of the mixture was measured and recorded as 10.62. The compositions for 44 hours were: 0.4 M of sodium hydroxide, 4.99 g of cobalt acetate and 10.84 for pH. Acetic acid was used as a capping molecule to prepare the same type of nanoparticles using cobalt acetate. The compositions when cobalt acetate was used were: 0.7 M of sodium hydroxide and acetic acid of 2.40 g (with a density of 1.05 g/cm^3) and measured pH of 12.62. After the addition of cobalt acetate (4.99 g), the measured pH was 7.54.

2.5 Cobalt oxide nanoparticles from chemical precipitation with oxidation method using hydrogen peroxide

The method of synthesis was adopted from Yang *et al*. (2007) with some modification of heating the reaction. A hot plate was used as a source of heat in this project. A mass of 4.98 g cobalt acetate was dissolved in 10 mL of deionized water. Subsequently, 0.92 g of 30% H_2O_2 was dissolved in 10 mL of deionized water. Sodium hydroxide with a concentration of 0.3 M was dissolved in 100 mL of water in a flask. A 20 mL of 1-butanol was added to the flask. Thereafter sodium hydroxide solution was added to the cobalt acetate mixture. The solution

was placed in an oil bath and stirred with a magnetic stirrer at 85 °C for 16 hours. After cooling down to room temperature, the precipitate was collected by centrifugation at 5000 rpm for 5 minutes. The cleaning was done 3 times with 50 mL of 2M HCl, twice with 50 mL of de-ionized water then once with 50 mL of methanol. Then air dried in the fume hood for three days.

References

LEY, A. 2009. A spectroscopic and thermal study of cobalt carboxylates. University of the Witwatersrand, A dissertation submitted to the Faculty of Science, University of the Witwatersrand, in fulfillment of the requirements for the degree of Master of Science, 1-121.

RAJARATHNAM, D. 2014. Instrumental chemical analysis: basic principles and techniques. Department of Chemical and Biomolecular Engineering Faculty of Engineering, National University of Singapore, Classification of Analytical Techniques. Second edition, 4, 1-39.

SUN, C. SU, X. XIAO, F. NIU, C. & WANG, J. 2011. Synthesis of nearly monodisperse Co_3O_4 nanocubes via a microwave-assisted solvothermal process and their gas sensing properties. *Sensors and Actuators B,* 157, 681-685.

XU, R. & ZENG, H. C. 2004. Self-generation of tiered surfactants superstructures for one-pot synthesis of CoO nanocubes and their close and non-close-packed organization. *Langmuir,* 20, 9780-9790.

YANG, Y-P., LIU, R. S., HUANG, K-L., WANG, L. P., LIU, S-Q. & ZENG, W. W. 2007. Preparation and electrochemical performance of nanosized Co_3O_4 via hydrothermal method, *Transactions of Nonferrous Metals Society of China,* 17, 1334-1338.

CHAPTER 3: RESULTS AND DISCUSSIONS

3.1 Introduction

Cobalt oxide nanoparticles were prepared from cobalt complexes and salts. Carboxylic acids with different carbon chain lengths acetic acid i.e. (C_2), heptanoic acid (C_7) and stearic acid (C_{18}) (Figure 3 (a-c)) were used as ligands. Cobalt complexes namely cobalt acetate, cobalt heptanoate and cobalt stearate complexes (Figure. 3 (d-f)) were prepared using these organic acid ligands and cobalt carbonate was used as the source of cobalt. The influence of the chain lengths of the carboxylic acids on the synthesis of cobalt oxide nanoparticles was investigated. Various sizes of irregularly shaped nanoparticles were found. Elemental analysis (EA) from the cobalt acetate showed that the calculated and theoretical values of carbon and hydrogen did not match hence commercial cobalt acetate was used as the third complex and in the entire project. Due to solubility problems experienced during the dissolution of cobalt complexes, another method (chemical precipitation) was sought for the synthesis of cobalt oxide nanoparticles.

The chemical precipitation method, which involved oxidation using oxygen as an oxidant and sodium hydroxide as a precipitant was chosen as an alternative method of synthesizing cobalt oxide nanoparticles. The effect of the carboxylic group was investigated using cobalt acetate and cobalt nitrate as precursors. The two precursors were chosen from a derivative salt of the carboxylic group (cobalt acetate) and the other without the carboxylic group (cobalt nitrate). The reaction temperature was maintained between 80 and 85 ºC for 72 hours. The presence of the carboxylic group showed that it had an influence on the size and shape of cobalt oxide nanoparticles. Oxygen and hydrogen peroxide were compared with one another using cobalt

acetate. Hydrogen peroxide was found to be a better oxidant since it exhibited smaller particles. The reaction time was varied at 16, 44 and 72 hours to observe the growth process. The results showed the size of cobalt oxide nanoparticles were increasing with time. The effect of the precipitating agent was studied by varying the concentration (0.2, 0.3, 0.4, 0.7 M) using cobalt acetate as the precursor. The sizes of the particles were found to decrease as the concentration of NaOH was increased due to ionic strength. Mixtures of different shapes were observed when the concentration was increased further to 0.7 M of NaOH. Acetic acid was used as a capping molecule. The use of acetic acid as capping agent resulted in cubic shapes.

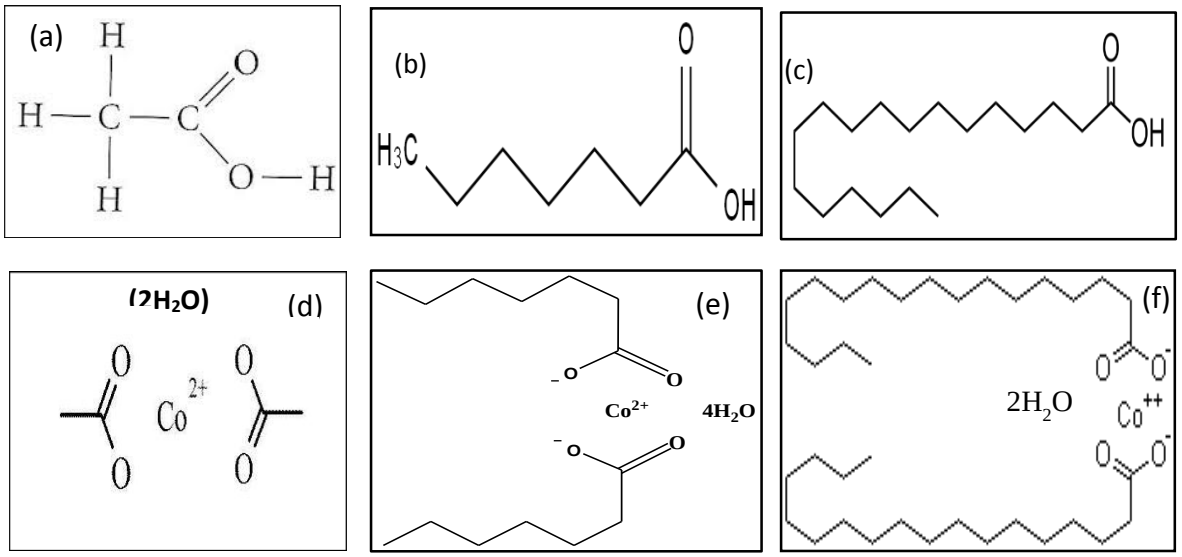

Figure 3: Structures of carboxylic acids: (a) acetic acid ($C_2H_4O_2$), (b) heptanoic acid ($C_7H_{14}O_2$), (c) stearic acid ($C_{18}H_{36}O_2$), (d) cobalt acetate ($Co(CH_3COO)_2.2H_2O$), (e) cobalt heptanoate ($Co(CH_3)(CH_2)_5COO)_2.4H_2O$), (f) cobalt stearate ($Co(CH_3(CH_2)_{16}COO)_2.\ 2H_2O$.

3.2 Synthesis and characterization of cobalt complexes

3.2.1 Elemental analysis (carbon and hydrogen) of the cobalt complexes

The carbon and hydrogen elemental compositions of the complexes are shown in Table 1. The calculated and the theoretical values from cobalt heptanoate, cobalt stearate and the commercial cobalt acetate were similar. This was indicative of the successful formation of the complexes. However, the theoretical and calculated compositions of the prepared cobalt acetate were different. The experimental and calculated carbon was 15.14 and 22.54%, respectively. The hydrogen content was 2.69 and 4.69% for experimental and calculated values respectively. This could be due to a complete dissociation of the acetic acid used in the preparation of cobalt acetate (Kusrini *et al*. 2013).

Table 1: Elemental analysis (carbon and hydrogen) for cobalt complexes

Complexes	**Carbon (C), %**		**Hydrogen (H),%**	
	Theoretical	Calculated	Theoretical	Calculated
$Co(CH_3COO)_2.2H_2O$-prepared	15.14	22.54	2.69	4.69
$Co(CH_3COO)_2.4H_2O$-commercial	19.35	19.29	5.60	5.68
$Co[(CH_3)(CH_2)_5COO]_2.4H_2O$	43.33	43.32	8.71	8.76
$Co[CH_3(CH_2)_{16}COO]_2.2H_2O$	65.96	65.32	10.99	10.66

3.2.2 Thermal analyses of cobalt complexes

The thermal decomposition and stability of the metal complexes were investigated using TGA in a nitrogen environment. The TGA and DTA curves are shown in Figure 4. The TGA in Figure 4A shows that there are several weight loss steps from the cobalt complexes. The curves

show that the greatest weight loss was from cobalt stearate at 92% followed by cobalt heptanoate at 68% and the commercial cobalt acetate at 59% and 42% from the prepared cobalt acetate. This was because shorter chains give lower thermal stability (Yin *et al*. 2004). The total weight losses of the complexes increased as the carbon chain length of the carboxylic acid increased. The final decomposition temperature of the prepared cobalt acetate was at 421 °C and the commercial cobalt acetate was 363 °C respectively. Cobalt heptanoate and cobalt stearate decomposition temperatures were at 382 and 446 °C respectively. The final decomposition temperature of cobalt acetate (prepared) was expected to be lower than that of cobalt heptanoate due to the size of the acetate. Thus, commercial cobalt acetate decomposition temperature is more effective. The decomposition temperature increased as the chain length of complexes increase (excluding the temperature from the prepared cobalt acetate.

Yin *et al*. (2004) observed that the presence of carboxylic acids influenced the decomposition temperature during the synthesis of iron oxide nanoparticles. Their study showed that the decomposition temperature increased as the length of the carboxylic acids increases. Short hydrocarbon chain carboxylates usually decompose at solid state whilst the longer chains decompose from the melt (Schneller *et al*. 2013). Figure 4B shows the derivative curves of Figure 4A. The DTA curve from the commercial cobalt acetate showed three decomposition steps. The first decomposition took place at 77 °C due to water of crystallization with a weight loss of 14%. The second weight loss was observed at 272 °C due to CH_2OH and the third weight loss at 356 °C due cobalt oxide (CoO) formation. The prepared cobalt acetate shows a loss of 2% due to water at 75 °C. The second weight loss of 13% was observed at 278 °C due to CH_2OH and the third weight loss of 32% at 351 °C was due to the formation of cobalt oxide.

Nevertheless, the TGA findings and those from the elemental analyses motivate the usage of commercial cobalt acetate for further investigations.

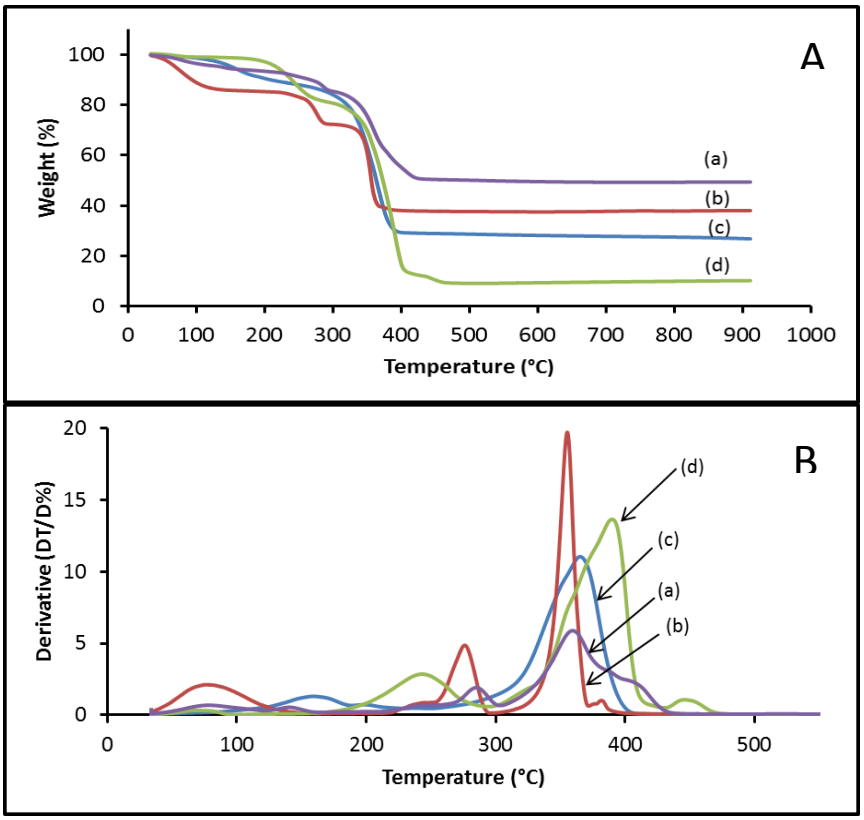

Figure 4: TGA (A) and DTA (B) profiles of (a) cobalt acetate (prepared), (b) cobalt acetate (commercial), (c) cobalt heptanoate and (d) cobalt stearate complexes.

Cobalt heptanoate showed a small weight loss of 2% at 109 °C while the second and the last decomposition steps were observed at 155 °C with 9% loss and 364 °C with 57% loss respectively. The first weight loss was attributed to some residual moisture in the sample. The second decomposition was due to organics and the last step was indicative of CoO formation. Cobalt stearate had four decomposition steps. The first step was at 67 °C showed 1% loss. The second step with a weight loss of 15% at 229 °C was due to organics from the carbon chain. The third step with 70% weight loss at 385 °C was attributed to the formation of CoO and the fourth step at 443 °C with 6% weight loss.

3.2.3 FTIR spectroscopy of cobalt complexes

Figure 5 shows the FTIR spectra of the commercial cobalt acetate, cobalt heptanoate, and cobalt stearate complexes. All complexes showed peaks associated with the carboxylate group of the asymmetric COO^- peaks at 1523, 1568, and 1556 cm^{-1}. These peaks were from the commercial cobalt acetate, cobalt heptanoate, and cobalt stearate respectively. The symmetric COO^- peaks were observed at 1425 cm^{-1} (commercial cobalt acetate), 1420 cm^{-1} (cobalt heptanoate) and 1414 cm^{-1} (cobalt stearate). The absorption band associated with C=O stretch was observed at 1706 cm^{-1} from cobalt acetate, cobalt heptanoate and cobalt stearate with different intensities. The intensity of the C=O peak increased as the carbon chain length increased. The asymmetric CH_2 and symmetric CH_2 were observed at 2961 and 2876 cm^{-1} respectively from cobalt heptanoate and cobalt stearate. This was expected due to long hydrocarbon chain.

The complexes with the shorter hydrocarbon chain did not have the CH_2 peaks. The peak at 3496 cm^{-1} appeared in all complexes but it was more intense from the commercial complex. This peak was due to free hydroxyl (He *et al*. 2005) and O-H peak at 3191 cm^{-1} suggesting that the commercial cobalt acetate contains water of crystallization (Ley 2009). This was not observed from cobalt heptanoate and cobalt stearate. Two twin peaks were observed from cobalt heptanoate and cobalt stearate. These peaks were due to O-H interacting with the carbonate ions (Wang *et al*. 2015). To determine whether the reaction was successfully the two COO^- peaks were used. The results show that although the COO^- peaks were observed, there was also the C=O peak. This indicated that the complexes also contained some of the acid from the ligands.

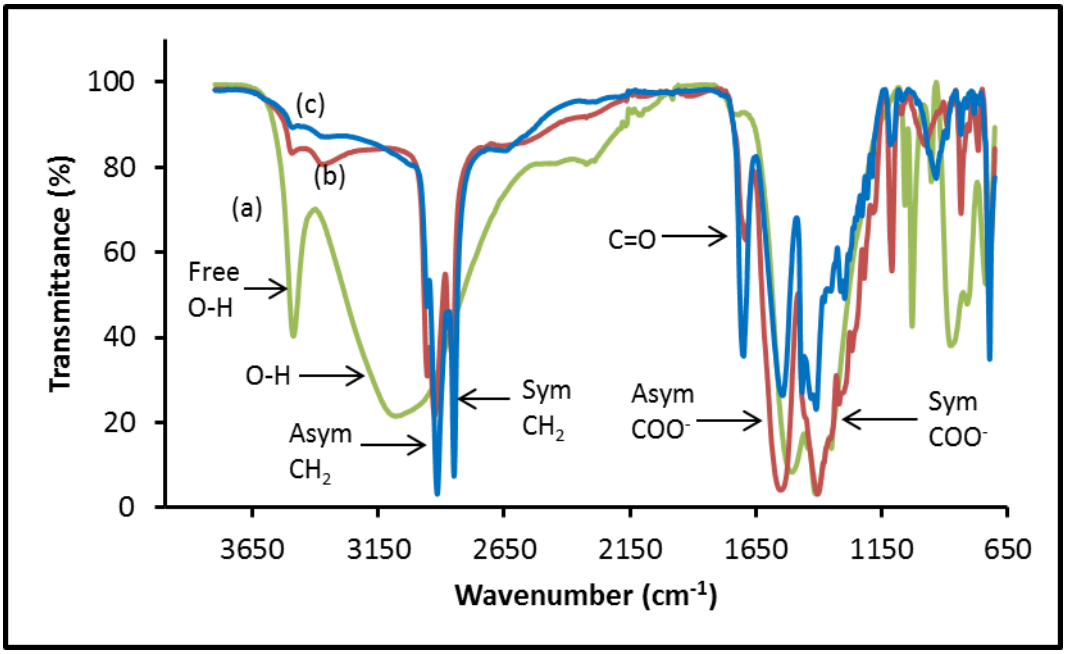

Figure 5: FTIR spectra of (a) commercial cobalt acetate (b) cobalt heptanoate and (c) cobalt stearate complexes.

3.3 Synthesis of cobalt oxide nanoparticles from cobalt acetate, cobalt heptanoate, and cobalt stearate complexes

A microwave-assisted technique was used to synthesize cobalt oxide nanoparticles from commercial cobalt acetate, cobalt stearate, and cobalt heptanoate complexes. No oxidizing agent was used but a mixture of 1-octadecene and ethanol (ratio of 2:1) was used as a solvent in order to improve the solubility of the complexes. The formation of the nanoparticles through the reaction of complexes as well as their characterization is discussed in this section.

3.3.1 X-ray diffraction of cobalt oxide nanoparticles synthesized from cobalt complexes

The XRD pattern of the particles synthesized from cobalt acetate, cobalt heptanoate, and cobalt stearate complexes are shown in Figure 6. The synthesized particles had two phases. One phase was assigned to cobalt oxide centred cubic phase matching JCPDS number 01-078-1969 with 2θ values of 22.09°, 36.47°, 43.05°, 45.07° 52.66°, 57.66°, 65.64°, 70.18°, 77.49° and 81.76° corresponded to the diffraction of (111), (220), (311), (222), (400), (331), (422), (511), (531) and (440) crystal faces. The other phase was assigned to cobalt-basic-carbonate hydrate compound, $Co(OH)_{1.0}(CO_3)_{0.5}.0.11H_2O$ which was observed at 26.03°, 30,95°,33.50°, 38.79°, 40.16°, 48.93°, 60.08° and 62.93° with miller indices of (220), (300), (301), (340), (412) and (450) (JCPDS 48-0083). This was attributed to residual precursors. The cobalt basic carbonate phase was also reported by Wang *et al*. (2011) which what was found in this current. The XRD patterns in this study showed that the particles had low crystallinity due to the oxidation of Co^{2+} (Wang *et al.* 2011). More of the cobalt hydroxide carbonate peaks were observed from particles made from cobalt heptanoate and cobalt stearate.

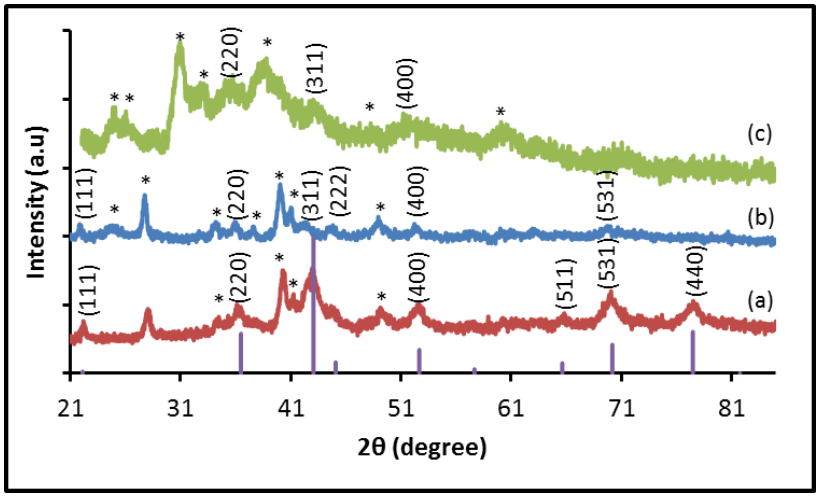

Figure 6: XRD pattern of cobalt oxide nanoparticles from (a) cobalt acetate, (b) cobalt heptanoate and (c) cobalt stearate complexes with (*) representing cobalt-basic-carbonate. The bars indicate the reference pattern of Co_3O_4 (JCPDS number 01-078-1969).

3.3.2 Morphological characterization of cobalt oxide nanoparticles synthesized from cobalt complexes

The TEM images and size distributions of the particles synthesized from cobalt acetate, cobalt heptanoate, and cobalt stearate complexes are shown in Figure 7. The particles from all complexes had a mixture of cube-like, rods, spheres and sheet-like shapes. Although the average sizes of the particles could not be determined due to mixed shapes, cobalt stearate seemed to yield bigger particles than cobalt acetate and cobalt heptanoate complexes. This could be as result of weak van der Waals forces as the length of hydrocarbon chain increases. Kodge *et al.* (2011) obtained irregular and spheres-like morphology during the decomposition of cobalt oxalate using the microwave technique in which high reaction temperatures were obtained by rapid microwave heating.

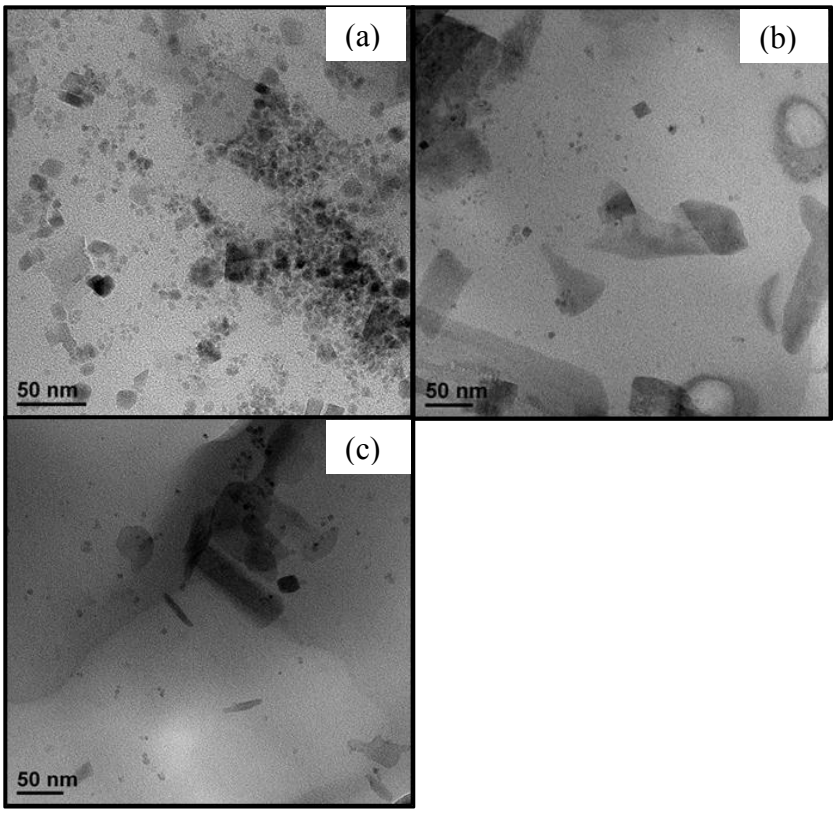

Figure 7: TEM images of cobalt oxide nanoparticles from (a) cobalt acetate, (b) from heptanoate and (c) from cobalt stearate.

3.3.3 FTIR spectroscopy of cobalt oxide nanoparticles synthesized from cobalt complexes

Figure 8 shows the FTIR spectra of cobalt oxide nanoparticles prepared from cobalt acetate, cobalt heptanoate, and cobalt stearate complexes. FTIR spectra show that there are peaks at 3194-3317 cm^{-1} assigned to the OH band from cobalt acetate suggesting that the compound contains water of crystallization. The broad peak could be as a result of hydrogen bonding between the acetate groups and the crystal water molecules (Ley 2009). Whilst nanoparticles from cobalt heptanoate and cobalt stearate showed multiple peaks in the same area of the OH band suggesting that there was the carbonate group. The asymmetric and symmetric CH_2 peaks were found at 2923 and 2854 cm^{-1} respectively. The intensity of the CH_2 peaks was increasing with the organic chain length of the complexes. This suggested that the organic part of the complexes were still present on the surface of the particles.

The peaks of interest were the characteristic double peaks due to asymmetric and symmetric COO^- stretch which was observed between 1539-1437 and 1412-1339 cm^{-1}. The presence of the COO^- groups means that there was a partial conversion of C=O to COO^-. Although the particles from cobalt heptanoate and cobalt stearate showed the presence of the carbonyl group (C=O) at 1706 cm^1 which was intense from the particles made from cobalt stearate. This suggested that there were traces of the starting materials. The C=O stretch was attributed to the presence of the free carboxylic acids (Ley 2009). The peaks COO^- peaks from cobalt heptanoate and cobalt stearate were broader. This might suggested that there was a possibility of multiple carboxylate bonding modes formed within the same structure (Ley 2009).

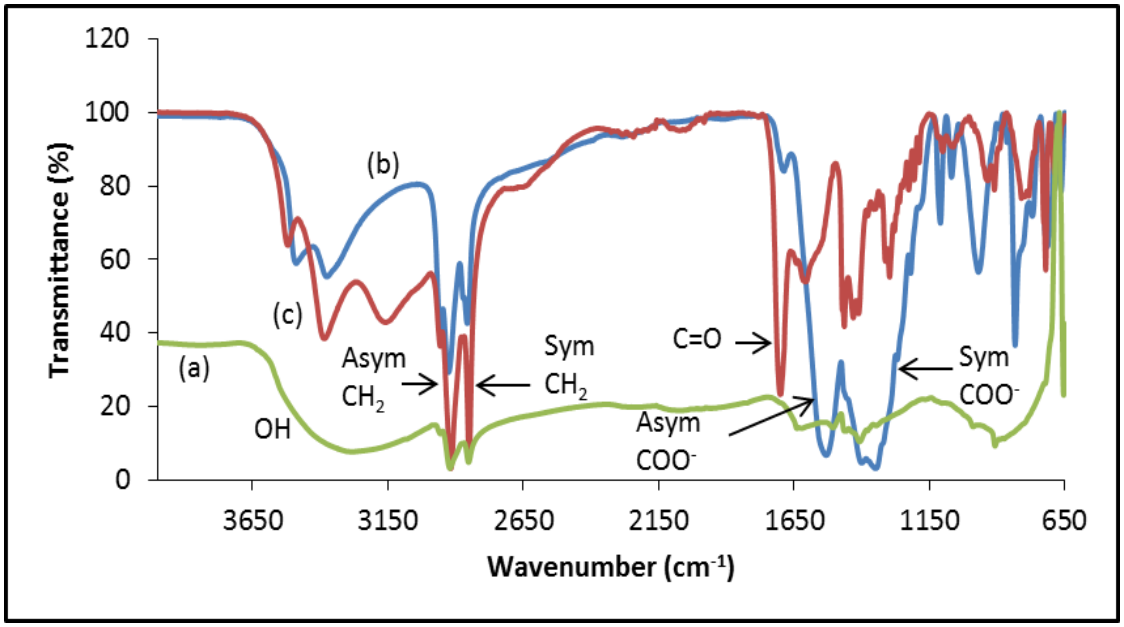

Figure 8: FTIR spectra of cobalt oxide nanoparticles from (a) cobalt acetate (b) cobalt heptanoate and (c) cobalt stearate.

3.3.4 Optical properties of cobalt oxide nanoparticles synthesized from cobalt complexes

Cobalt acetate, cobalt heptanoate and cobalt stearate complexes were analysed for their optical properties via UV-vis and photoluminescence spectroscopies. Their results are shown on Figure 9. The nanoparticles showed first peaks associated with the transition $\pi \rightarrow \pi^*$ (Al-Tuwirqi *et al.* 2011) at 220, 240, 245 nm from cobalt acetate, cobalt heptanoate and cobalt stearate respectively. The second peaks were observed at 430 nm due to the transition $^4T_{1g}$ (F) $\rightarrow$ $^4T_{1g}$ (p), for the octahedral Co^{2+} structure (Abdelrazek & Elashmawi 2008). The emitted peaks of the nanoparticles (Figure 9 B) were observed at 734 nm from all compounds with excitation wavelength at 575 nm. The excitation wavelength chosen in the study gave the most intense emission peak for the nanoparticles; hence this wavelength was used throughout this project. Wang & Xu (2015) obtained a broad peak emission peak at 710 nm for nanoplates which was attributed to indirect optical band gap emission.

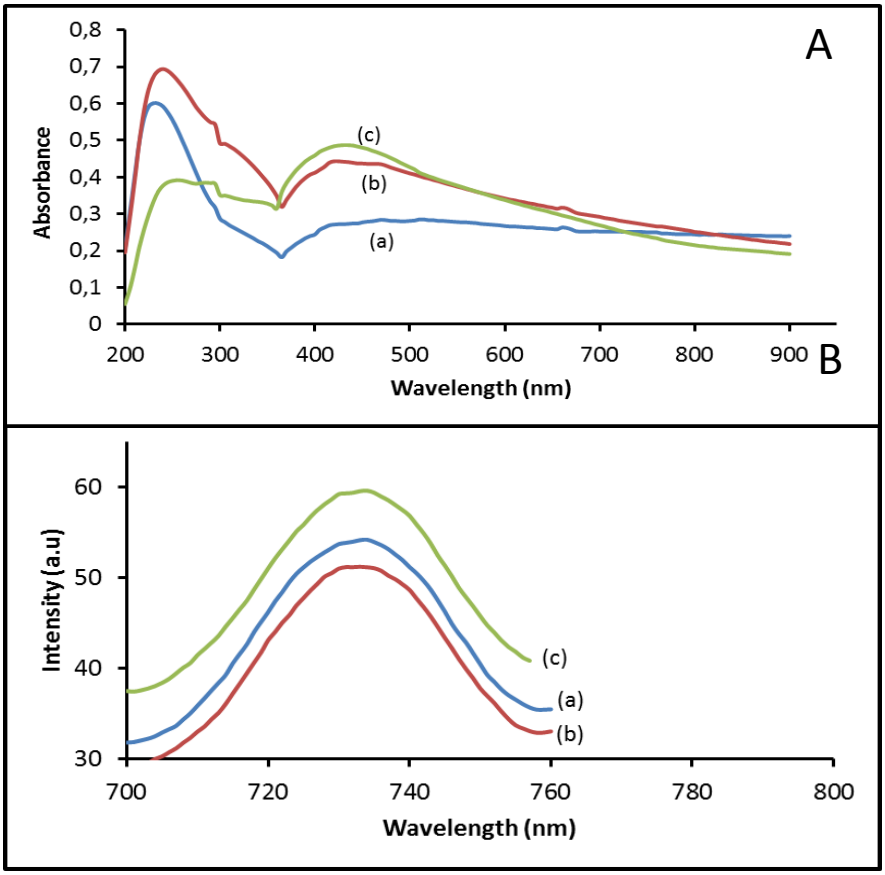

Figure 9: Absorption (A) and emission spectra (B) of cobalt oxide nanoparticles from (a) cobalt acetate, (b) cobalt heptanoate and (c) cobalt stearate.

3.4 Synthesis of cobalt oxide nanoparticles prepared using chemical precipitation method

The nanoparticles were prepared using precipitation method in the presence of an oxidant (O_2 and H_2O_2) and precipitating agent, NaOH. Different parameters such as acetate, oxidant, time and NaOH were studied. Acetic acid was also introduced as the capping molecule while using different precursors (cobalt acetate and cobalt nitrate).

3.4.1 Effect of acetate ion on cobalt oxide nanoparticles

In order to study the effect of acetate ion on the properties of cobalt oxide nanoparticles cobalt acetate and cobalt nitrate were the two different precursors used. The two precursors were chosen in order to compare the nanoparticles made from the acetate and one without the acetate group. The synthesized particles using O_2, at 85 °C for 72 hours and 0.3 M (moles per 100 mL of water used) of NaOH were characterised and the results are presented and discussed below.

3.4.1.1 X-ray diffraction of cobalt oxide nanoparticles synthesis from $Co(CH_3COO)_2$ and $Co(NO_3)_2$ precursors

The crystalline diffraction properties of the nanoparticles prepared from cobalt nitrate and cobalt acetate precursors are shown in Figure 10. Eight peaks were observed at 2θ values of 22.18°, 36.61°, 43.21°, 45.24°, 52.73°, 65.90°, 70.31° and 77.42° which correspond to the diffraction indices of (111), (220), (311), (222), (400), (422), (511) and (440) planes respectively. They are indexed to face-centered cubic phase (fcc**)** of cobalt oxide (JCPDS number 01-065-3103). This confirmed that the synthesized nanoparticles were made of cobalt oxide from both precursors. However, two minor peaks were found at 23.13° and 38.49° in the nanoparticles prepared from cobalt nitrate which were due to cobalt oxide hydroxide, CoOOH which was an intermediate compound before the final product cobalt oxide phase. The sharp peaks from cobalt nitrate suggested high crystallinity and large nanoparticles (Kang and Zhou 2015). The most intense peak, which is at 2θ of 43.12°, was used to calculate the size of the nanoparticles as per Debye Scherer equation (Equation 1). The average sizes of cobalt oxide nanoparticles were 13 nm and 9 nm when the precursors were cobalt nitrate and cobalt acetate respectively. Smaller sized particles obtained from cobalt acetate indicated that the acetate group played a role of capping the nanoparticles for better growth.

$D = 0.9 \lambda / (B \cos \theta)$ Equation 3

Where:

d is Average crystal size,

λ is Wavelength of incident beam ($CuK\alpha_1$ at 1.54060Å),

β is FWHM in radians,

θ is Scattering angle in degree

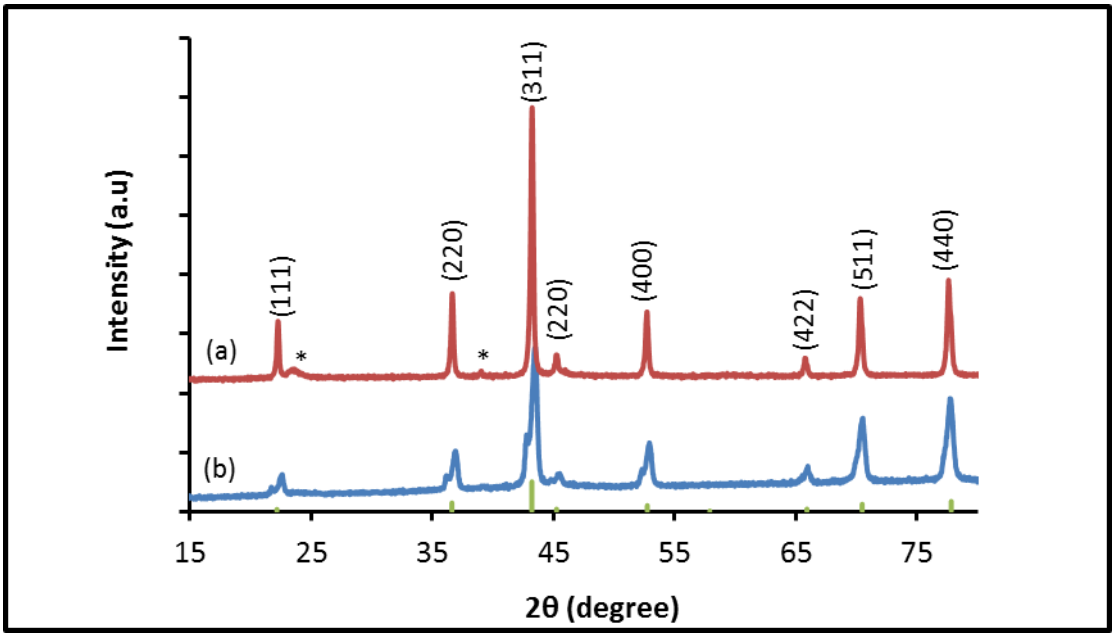

Figure 10: XRD pattern of cobalt oxide nanoparticles from (a) cobalt nitrate and (b) cobalt acetate precursors with (*) representing the less dominant phase. The bars indicate the reference pattern of Co_3O_4 (JCPDS number 01-065-3103).

3.4.1.2 Morphological characterization of cobalt oxide nanoparticles synthesis from $Co(CH_3COO)_2$ and $Co(NO_3)_2$ precursors

The TEM images and the size distribution of the Co_3O_4 nanoparticles prepared from cobalt nitrate and cobalt acetate precursors are shown in Figure 11. The cobalt oxide nanoparticles prepared from cobalt nitrate were spherical-like while those from cobalt acetate were cubic. The cause for different morphologies might be due to different precipitation compositions from the nitrate and the acetate (Yang *et al.* 2007). The average sizes were 82.10 nm (standard deviation 35.91) and 35.70 nm (standard deviation 23.44) for nanoparticles synthesized from cobalt nitrate and cobalt acetate respectively. The average sizes of the nanoparticles prepared from cobalt acetate are smaller compared to the nanoparticles synthesized from cobalt nitrate. A narrow size distribution of cobalt oxide nanoparticles was obtained when the precursor was changed from cobalt nitrate to cobalt acetate. This indicated that the acetate effectively controlled the growth of the particles and reduced their size. The decrease in size might be due to the acetate group adsorbing on the surface of the nanoparticles and thus favouring a better growth. Therefore, the anion type might have played an important role in determining the size and the shape of cobalt oxide.

The sizes calculated from XRD were small as compared to TEM sizes, although the trend was similar in that the nanoparticles from cobalt acetate were smaller. TEM measures each and every particle in the sample in 2D. Hence the results from XRD showed smaller sizes. The sizes calculated from TEM results were used throughout this project. Yang *et al.* (2007) studied the effect of cobalt sources using cobalt acetate and cobalt nitrate as precursors. H_2O_2 was used as an oxidant. Their results showed that sphere-like cobalt oxide nanoparticles were obtained when using cobalt nitrate whilst cubic shape was formed from cobalt acetate. It was concluded that the shape of cobalt oxide nanoparticles was controlled by altering the precursor salts.

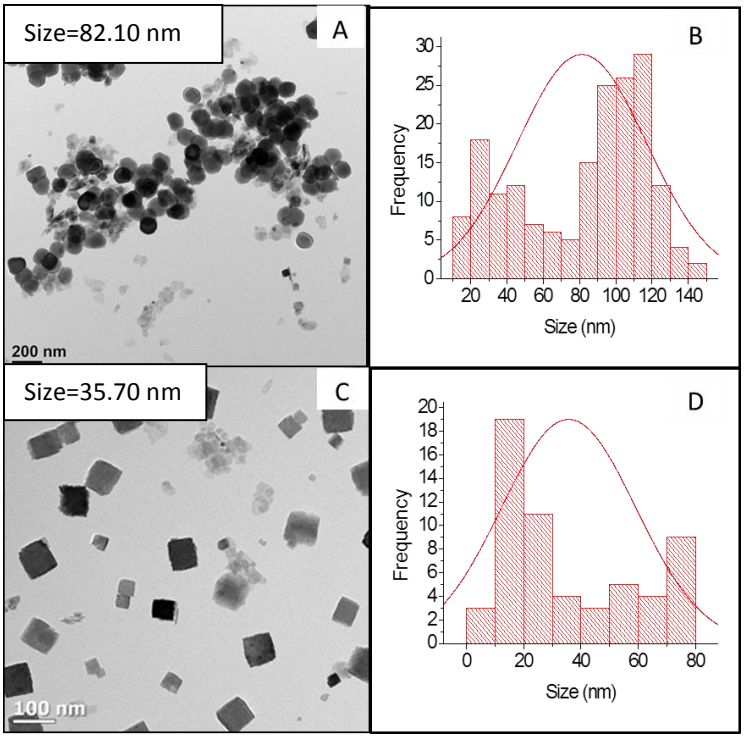

Figure 11: TEM and size distribution of cobalt oxide (a) and (b) from cobalt nitrate and (c), (d) from cobalt acetate.

3.4.1.3 FTIR spectroscopy of cobalt oxide nanoparticles synthesis from $Co(CH_3COO)_2$ and $Co(NO_3)_2$ precursors

The FTIR spectroscopy was used to characterize Co_3O_4 nanoparticles synthesized from cobalt nitrate and cobalt acetate precursor. The FTIR spectra are shown in Figure 12. The peaks observed at 1541 and 1427 cm^{-1} were due to the COO^- asymmetric and COO^- symmetric stretches respectively when cobalt acetate was used as the precursor. These peaks were not found in the nanoparticles synthesized from cobalt nitrate. The presence of the COO^- groups was an indication that the reaction was successful hence there was an absence of the carbonyl group (C=O) around 1700 cm^{-1}. The O-H stretches were observed at 3346 and 3365 cm^{-1} for

the nanoparticles prepared from cobalt nitrate and cobalt acetate respectively. The OH peaks were an indication that the samples contained the water of crystallization (Ley 2009).

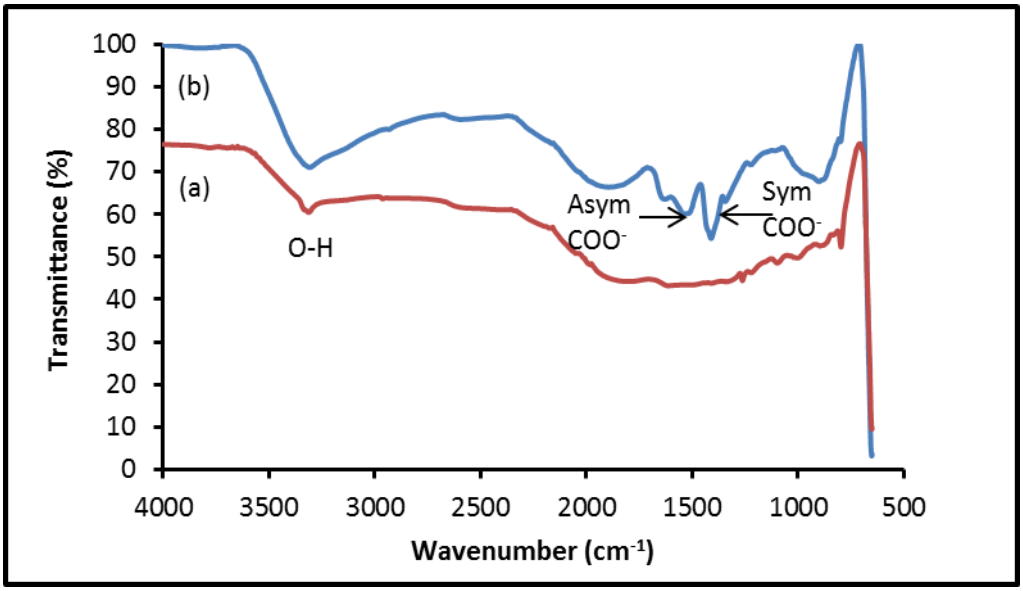

Figure 12: FTIR spectra of cobalt oxide nanoparticles from (a) cobalt nitrate and (b) cobalt acetate.

3.4.1.4 Optical properties of cobalt oxide nanoparticles synthesis from $Co(CH_3COO)_2$ and $Co(NO_3)_2$ precursors

The optical properties of the cobalt oxide nanoparticles using cobalt nitrate and cobalt acetate precursors are shown in Figure 13. Three absorption peaks were observed from nanoparticles synthesized from both precursors. The $\pi \rightarrow \pi^*$ absorptions were 275 and 271 nm from nanoparticles prepared using cobalt nitrate and cobalt acetate respectively. The transition due to $^4T_{1g}$ (F) $\rightarrow$ $^4T_{1g}$ (p) were observed at 465 and 433 nm were due to particles from cobalt nitrate and cobalt acetate respectively. The peaks at 765 and 755 were due to $t_2g(Co^{3+}) \rightarrow t_2(Co^{2+})$ (Thota *et al*. 2009) from particles made of cobalt nitrate and cobalt acetate respectively. Multiple UV-vis peaks resulted from having multiple allowed transitions state of a molecule.

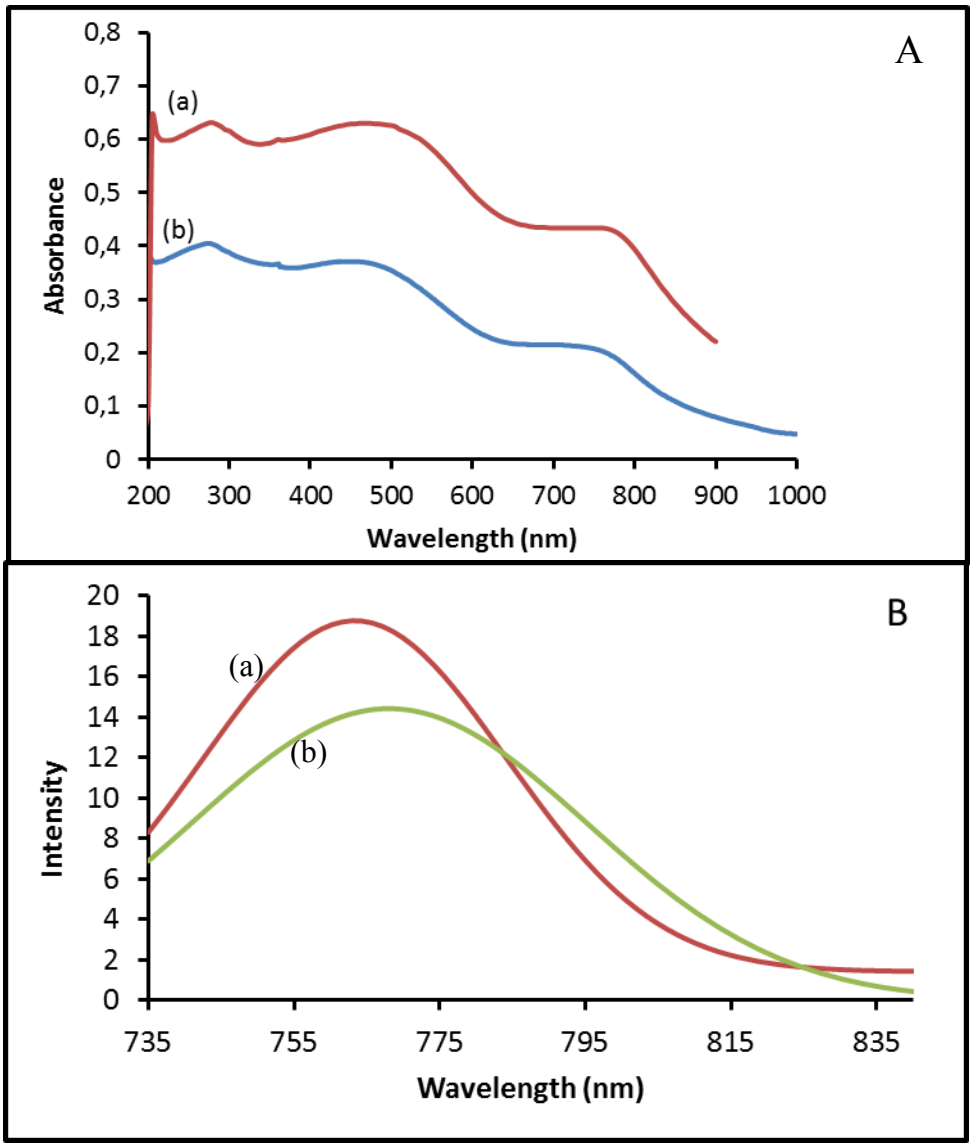

Figure 13: Absorption (A) and emission spectra (B) of cobalt oxide nanoparticles from (a) cobalt nitrate and (b) cobalt acetate precursors.

The bulk of Co_3O_4 is 566 and 838 nm (Niasari *et al*. 2009). The peaks at 465 and 433 nm were related to 566 nm from the bulk cobalt oxide whilst the values at 765 and 755 nm were associated with 838 nm of the bulk. The peaks from the nanoparticles from both precursors were blue shifted related to bulk of cobalt oxide. This indicated a decrease in size due to quantum confinement. The absorption peaks from particles made from cobalt acetate were shifted to lower wavelength compared to the one from cobalt nitrate which suggested that the

nanoparticles prepared using cobalt acetate were smaller compared to the ones from cobalt nitrate. This was in agreement with the TEM results. The emission spectra from both precursors are shown in Figure 13 (B). The emission maxima were found to be 768 and 762 nm from cobalt nitrate and cobalt acetate respectively. This is in agreement with the TEM and UV-vis results in that the nanoparticles prepared from cobalt acetate were smaller from the ones prepared from cobalt nitrate hence the emission peak is emitted at lower wavelength. These emission peaks are associated with the absorption peaks at 765 and 755 nm from particles made from cobalt nitrate and cobalt acetate respectively. Hence only one peak of emission was observed. The emission peaks of the particles from both precursors were red shifted compared to the absorption peaks.

3.4.2 Effect of oxidant on the synthesis of cobalt oxide nanoparticles

The effect of the H_2O_2 and O_2 was investigated during the synthesis of the cobalt oxide nanoparticles. Oxygen and hydrogen peroxide were compared with one another as oxidant necessary to oxidize the Co^{2+} in $Co(OH)_2$ to Co^{3+} (Teng *et al*. 2010) using cobalt acetate. The other parameters were kept constant namely, the temperature of 85 °C and 0.3 M of NaOH. Cobalt acetate was used as the precursor. The reaction time using oxygen was 72 hours and 16 hours when hydrogen peroxide was used. The reaction time using H_2O_2 showed the formation of cobalt oxide was faster compared to using oxygen.

3.4.2.1 X-ray diffraction of cobalt oxide nanoparticles synthesized using oxygen and hydrogen peroxide

Figure 14 shows the XRD pattern of the cobalt oxide nanoparticles using oxygen and hydrogen peroxide. The diffraction peaks from all samples were observed at 2θ values of 22.18°, 36.01°, 43.22°, 45.24°, 52.74°, 65.91°, 70.47° and 77.82° which correspond to the indices of (111), (220), (311), (222), (400), (422), (511) and (440) detailing a face-centered cubic phase (fcc) of cobalt oxide (JCPDS number 03-065-1303). The peaks from nanoparticles synthesized using H_2O_2 were broad which was indicative of smaller sizes. Hence the peak at 45.24° and 66.15° showed that might have overlapped with the peak at (311) and (511) index peak respectively or it might have been due to low phase of cobalt oxide.

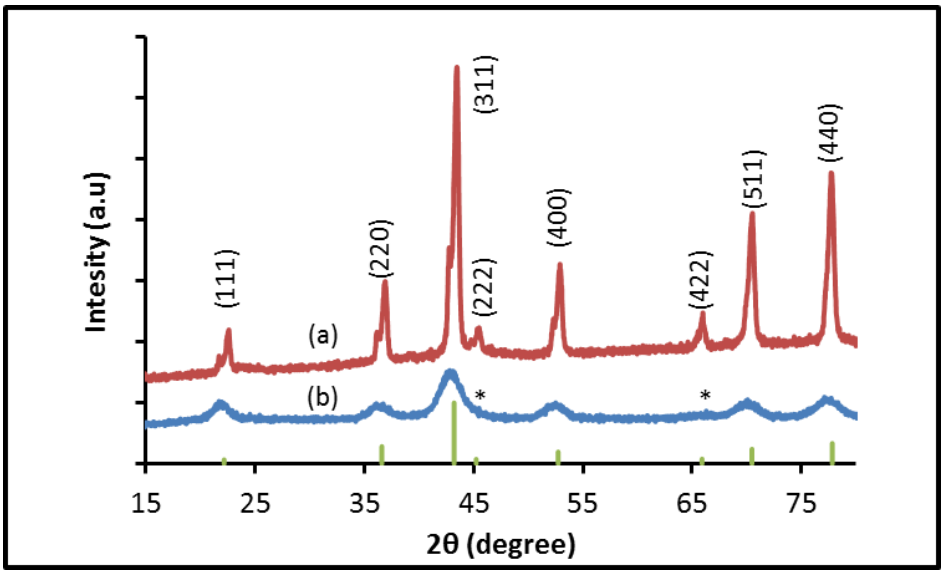

Figure 14: XRD pattern of cobalt oxide nanoparticles using (a) oxygen and (b) hydrogen peroxide. The bars indicate the reference pattern Co_3O_4 (JCPDS number 03-065-1303).

3.4.2.2 Morphological characterization of cobalt oxide nanoparticles synthesized using oxygen and hydrogen peroxide

The morphology and size distribution of cobalt oxide nanoparticles are shown in Figure 15. The morphology of cobalt oxide nanoparticles was cubic from both oxidants. The size distribution of both oxidants is shown in Figure 15 B and D. The size distribution of particles when using hydrogen peroxide was narrower compared to the use of oxygen. The average sizes of the nanoparticles were 35.70 nm (standard deviation 23.44) and 4.45 nm (standard deviation 1.05) using oxygen and hydrogen peroxide respectively. The nanoparticles prepared from H_2O_2 were smaller compared to those synthesized from oxygen. The results agreed with the observation made in section 3.4.2.1 (XRD results). The smaller sizes were due to hydrogen peroxide being stronger oxidant and faster reaction rate compared to oxygen. Nanoparticles synthesized using oxygen took place under thermodynamic control where slow growth rate and longer reaction time were favored growth of the nanoparticles. In the presence of hydrogen peroxide, the reaction favored kinetic conditions where the reaction rate was fast and therefore the particle sizes were reduced.

Casillas *et al.* (2012) suggested that formation of a large number of small particles was due to a large number of nuclei formed at a fast rate during the nucleation stage. Whilst the formation of large particles was due to slow growth of the nuclei hence there were few particles formed because the rate was slow. The nanoparticles obtained from oxygen showed that a surface wrapping growth mechanism (Feng & Zeng 2003) was taking place. Surface wrapping happens when the growth is not taking place layer by layer. This happens when the nucleation and growth take place simultaneously (Feng & Zeng 2003). Xu & Zeng 2003 used oxygen in the synthesis of cobalt oxide nanoparticles at 95° for 74 hours. The authors obtained the nanoparticles in cubic morphology with a size of 47 nm when using 90 g of sodium nitrate to

mediate the synthesis of cobalt oxide nanoparticles. The larger particles obtained in their study might be due to the use of higher temperature compared to the temperature used in this study. Yang *et al.* (2007) synthesized cubic cobalt oxide for 16 hours using an autoclave from cobalt acetate and obtained small particles with an average size of 20 nm when hydrogen peroxide was used as an oxidant.

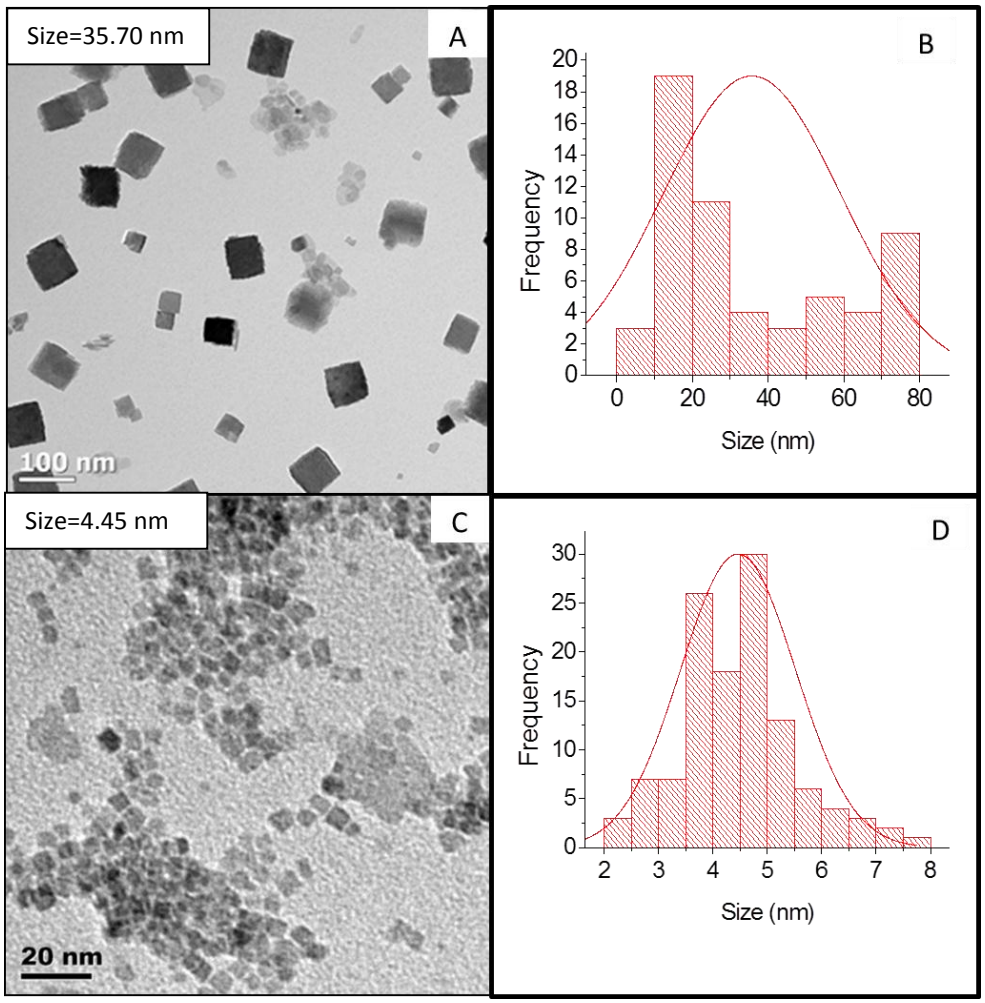

Figure 15: TEM and size distribution of cobalt oxide nanoparticles using (a) and (b) oxygen then (c) and (d) hydrogen peroxide.

3.4.2.3 FTIR spectroscopy of cobalt oxide nanoparticles synthesized using oxygen and hydrogen peroxide

The FTIR spectra of the cobalt oxide nanoparticles synthesized from cobalt acetate as a precursor and using oxygen and hydrogen peroxide as oxidants are shown in Figure 16. The main functional groups on the surface of the nanoparticles were O-H, COO^- asymmetric, and COO^- symmetric peaks from both oxidants. The peaks of the nanoparticles from both oxidants were observed at 3325, 1541 and 1536 cm^{-1} respectively. The use of hydrogen peroxide showed that they carboxylate groups were adsorbing strongly on the surface of cobalt oxide nanoparticles from the peak intensity. Formation of cubic morphology might be due to the presence of COO^- groups on the surface of the nanoparticles.

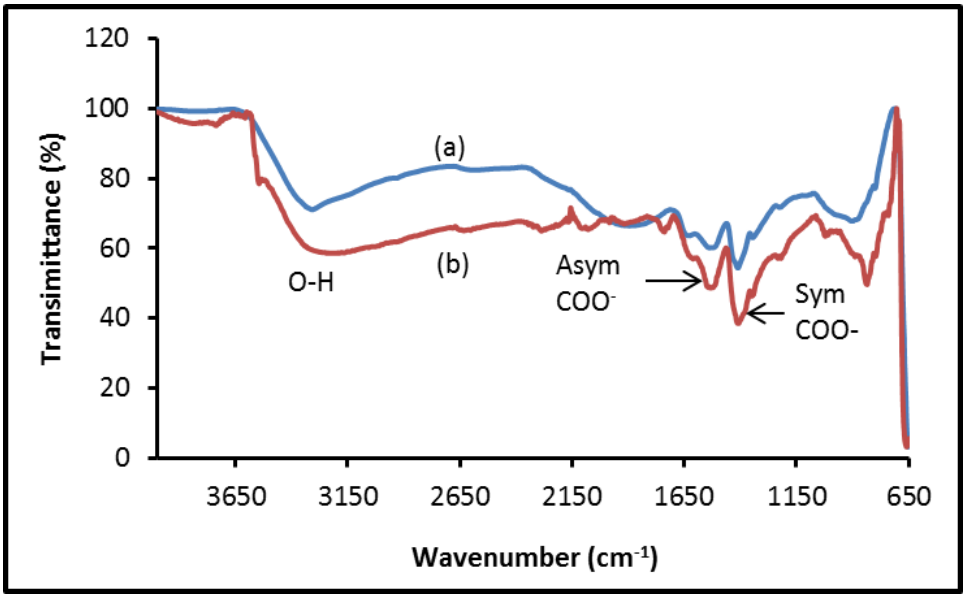

Figure 16: FTIR spectra of cobalt oxide nanoparticles using (a) oxygen and (b) hydrogen peroxide.

3.4.2.4 Optical properties of cobalt oxide nanoparticles synthesized using oxygen and hydrogen peroxide

The UV-vis absorption spectra of cobalt oxide nanoparticles synthesized from oxygen and hydrogen peroxide are shown in Figure 17A. The nanoparticles from both oxidants showed three absorption wavelengths at 271 nm, 433 nm and 755 nm from nanoparticles prepared using oxygen whilst the nanoparticles prepared using hydrogen peroxide showed absorption peaks at 390 nm, 680 nm, and 970 nm. The absorption wavelengths of nanoparticles prepared using hydrogen peroxide were observed at higher wavelengths compared the ones prepared using oxygen. This might be due to a surface defect of extremely small particle sizes. Hence the emission peak at Figure 17B is also red shifted at 776 nm from nanocubes using H_2O_2 compared to the ones using oxygen at 772 nm.

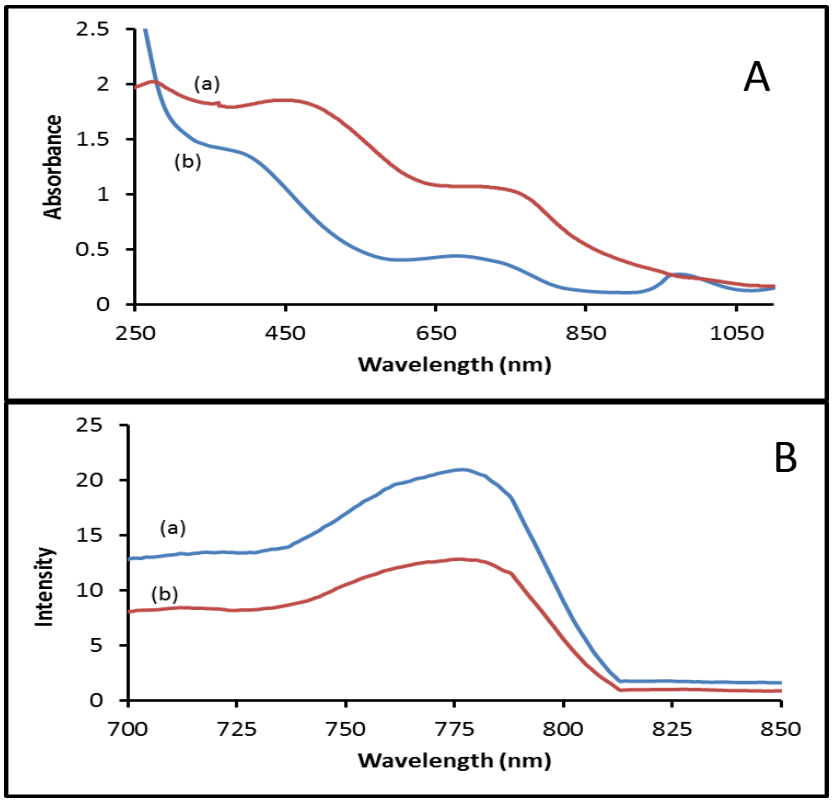

Figure 17: Absorption (A) and (B) emission spectra of cobalt oxide nanoparticles using (a) oxygen and (b) hydrogen peroxide.

3.4.3 Effect of time on the synthesis of cobalt oxide nanoparticles

In this section, cobalt acetate was used as the precursor in the presence of 0.4 M NaOH at 85 °C for 72 hours and oxygen as an oxidant. The time is considered as one of the parameters which have an influence on the size of the nanoparticles. Therefore, the effect of time was studied by synthesizing the nanoparticles for 16, 44 and 72 hours.

3.4.3.1 X-ray diffraction of cobalt oxide nanoparticles synthesized at 16, 44 and 72 hours

Figure 18 shows the XRD pattern of the obtained cobalt oxide nanoparticles synthesized at different times (16, 44 and 72 hours). All peaks with their corresponding 2θ values were indexed to face-centered cubic phase (fcc) of cobalt oxide (JCPDS number 03-065-1303). The diffraction peaks from all samples were sharp, which are indicative of high crystallinity. No crystalline peaks corresponding to impurities were detected.

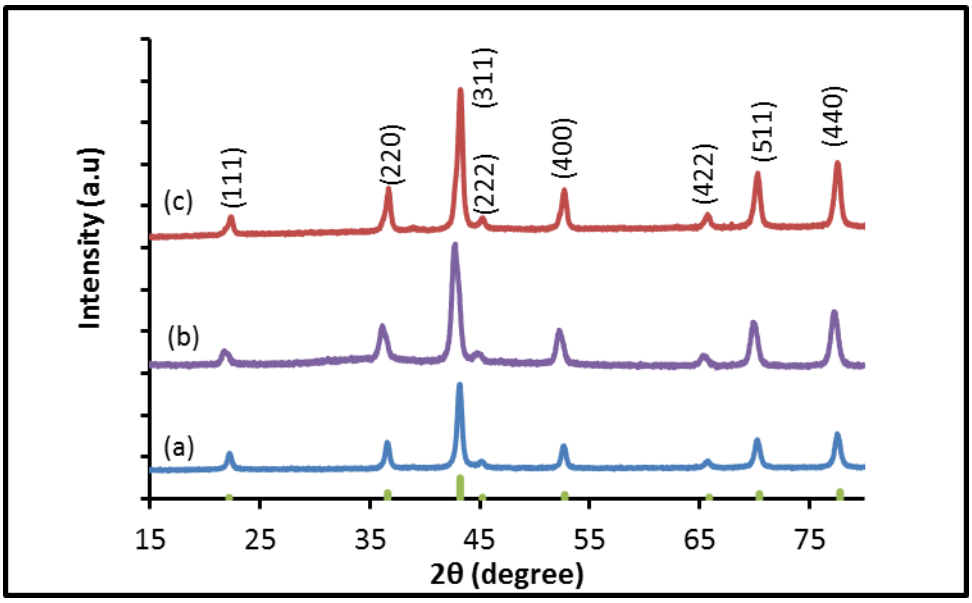

Figure 18: XRD pattern of cobalt oxide nanoparticles synthesized for (a) 16 hours, (b) 44 hours and (c) 72 hours. The bars indicate the reference pattern of Co_3O_4 (JCPDS number 03-065-1303).

3.4.3.2 Morphological of cobalt oxide nanoparticles synthesized at 16, 44 and 72 hours

The TEM images and the size distributions of the cobalt oxide nanoparticles synthesized at different times (16, 44 and 72 hours) are shown in Figure 19. The cobalt oxide nanoparticles from all samples were cubic in morphology. Their sizes were 22.81 nm (standard deviation 4.83), 23.81 nm (standard deviation 4.45) and 25.45 nm (standard deviation 6.12) at 16, 44 and 72 hours respectively. The size of the nanoparticles increased as the time increased. This suggested that cobalt oxide nanocubes were formed through the redissolving and redepositing process (Liu *et al*. 2005). Uniform morphology was also obtained as the time increased. This suggested that time was important in obtaining uniform nanocubes.

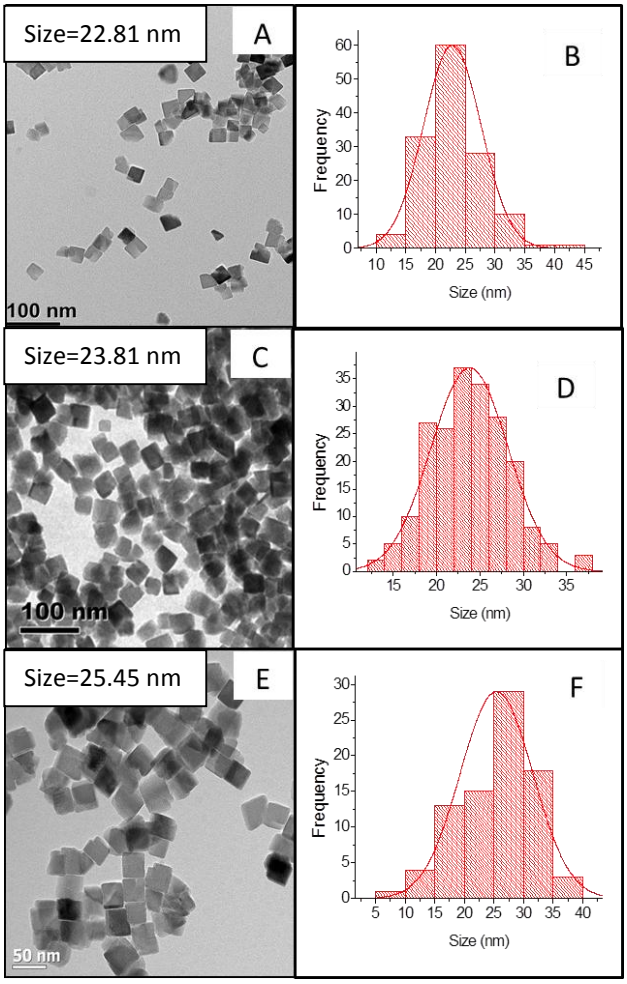

Figure 19: TEM and size distribution of cobalt oxide nanoparticles synthesized (a), (b) for 16 hours, (c), (d) for 44 hours and (e), (f) for 72 hours.

3.4.3.3 FTIR spectroscopy of cobalt oxide nanoparticles synthesized at 16, 44 and 72 hours

Figure 20 shows the FTIR spectra of the cobalt oxide nanoparticles prepared at different times (16, 44 and 72 hours). All samples exhibited a broad absorption band at 3411 cm^{-1} due to OH stretching vibration and H-OH at 1628 cm^{-1} due to bending modes of water. The asymmetric and symmetric COO^- peaks due to cobalt carboxylate were at 1440 and 1415 cm^{-1}. The O-H groups were due to the crystal water and C-H group which was due to the unreacted organic part from the precursor.

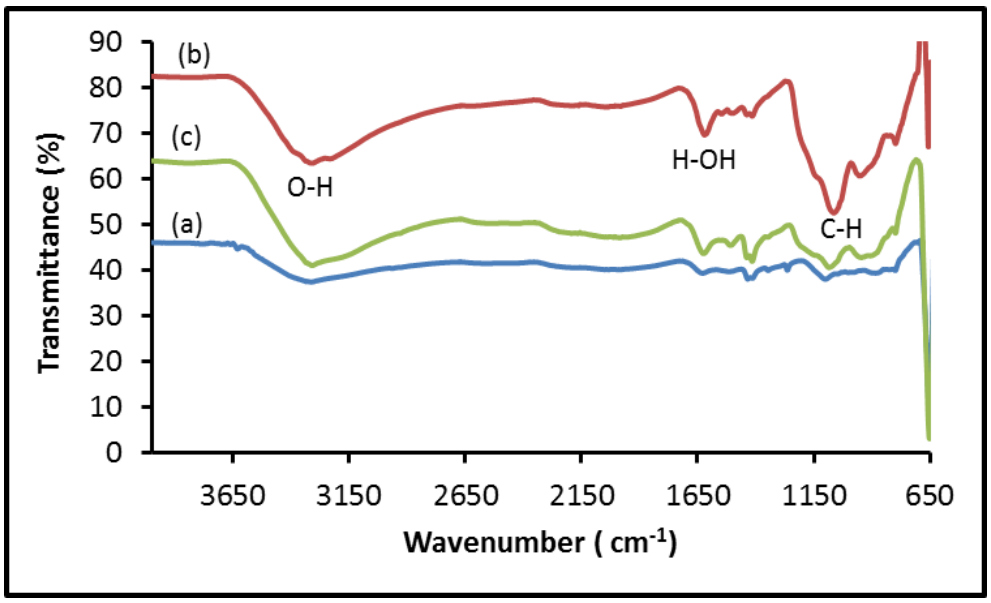

Figure 20: FTIR spectra of cobalt oxide nanoparticles synthesized for (a) 16 hours, (b) 44 hours and (c) 72 hours.

3.4.3.4 Optical properties of cobalt oxide nanoparticles synthesized at 16, 44 and 72 hours

Optical properties of the cobalt oxide nanoparticles at different times (16, 44 and 72 hours) are shown in Figure 21A. The UV spectra show that cobalt oxide nanoparticles had three absorption peaks. The particles synthesized at 16 hours gave an absorption spectrum with the peaks at the wavelengths of 205, 455 and 754 nm. The nanoparticles synthesized at 44 hours had absorption at 250, 460, 755 nm whilst the particles synthesized at 72 hours showed peaks

at 205, 470, 758 nm. The two peaks associated with the bulk from all samples showed that the absorption wavelength was increasing in the order 16, 44 and 72 hours. This was in agreement with TEM results. The emission peaks (Figure 21B) of cobalt oxide nanoparticles were 771 and 763 and 771 nm for the syntheses at 16, 44 and 72 hours respectively. There was no specific trend in the emissions results. This could be due to the fact that particle sizes were similar which were not too far apart.

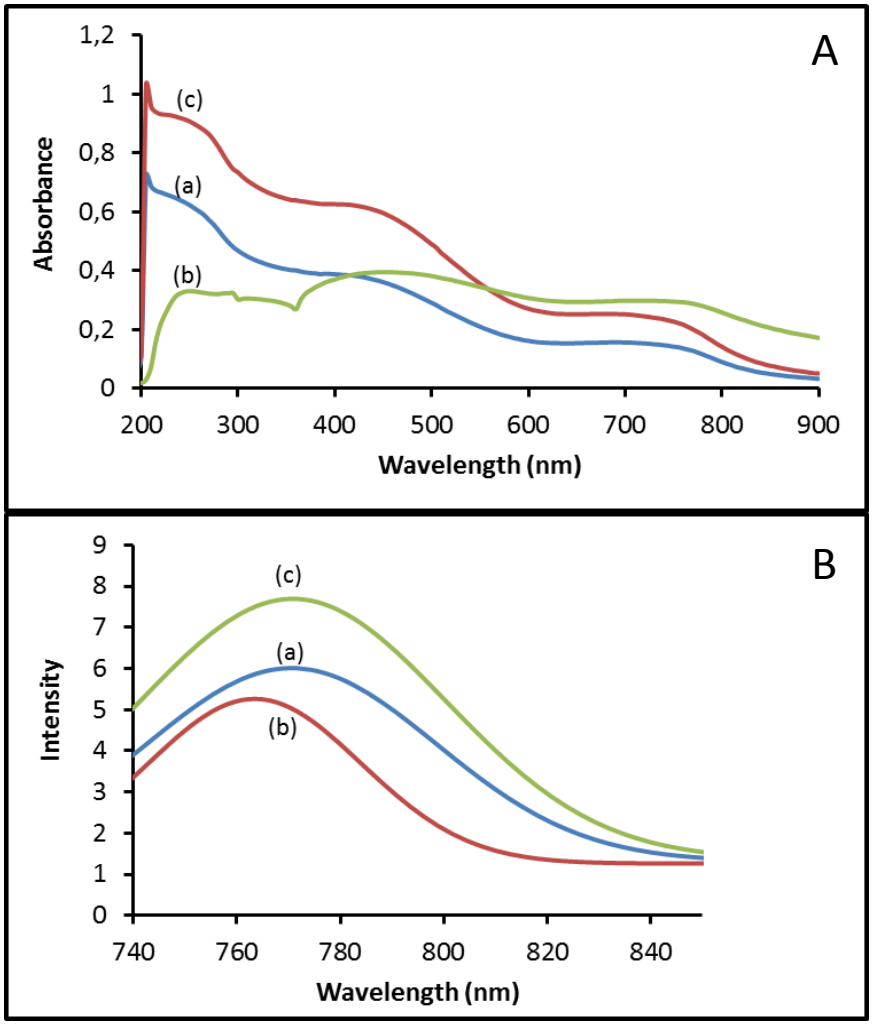

Figure 21: Absorption (A) and (B) emission spectra of cobalt oxide nanoparticles synthesized for (a) 16 hours, (b) 44 hours and (c) 72 hours.

3.4.4 Effect of sodium hydroxide concentration on the synthesis of cobalt oxide nanoparticles

In order to investigate the effect of the precipitating agent, the concentrations of NaOH were varied at 0.2, 0.3, and 0.4 and 0.7 M. Cobalt acetate was used as precursor and oxygen was used as the oxidant. The pH of the NaOH solutions were 7.9 8.5, 10.2 and 12.3 for concentrations of 0.2, 0.3, 0.4 and 0.7 M respectively.

3.4.4.1 X-ray diffraction of cobalt oxide nanoparticles synthesized at 0.2, 0.3, 0.4 and 0.7 M of sodium hydroxide

Figure 22 shows the diffraction pattern of cobalt oxide nanoparticles synthesized using NaOH at concentrations of 0.2, 0.3, 0.4 and 0.7 M. The diffraction for cobalt oxide nanoparticles prepared from 0.2, 0.3, 0.4 M of NaOH have similar peaks which were indexed to the cubic phase of cobalt oxide JCPDS number 03-065-1303. The particles synthesized from 0.7 M NaOH had a different pattern with peaks corresponding to JCPDS number 01-072-2280 of cobalt oxide hydroxide heterogenite (CoOOH) Rhombohedral phase. The formation of a different phase was due to a higher concentration of NaOH as this favored the formation of cobalt hydroxide under set conditions. The hydroxide tends to stabilize in the oxide hydroxide heterogenite through oxidation in the presence of dissolved oxygen in the solution or through dehydration. Similar findings were reported by Cui *et al*. (2013) with the alkaline solution pH set between 9 and 14. A solution with pH of 8-10 showed that it was suitable to obtain the cobalt oxide phase. An increase of NaOH concentration leads to an increase of $Co(OH)_2$ concentration which leads to the formation of CoOOH formation via $Co(OH)_2$ oxidation (Spataru *et al*. 2003). Cui *et al*. (2013) explained the formation of CoOOH saying that the when cobalt salt reacts with NaOH it will produce $Co(OH)_2$. The $Co(OH)_2$ will be oxidized to

$Co(OH)_3$ in the presence of oxygen in the solution. Then $Co(OH)_3$ will be dehydrated to CoOOH. The reactions below are the proposed mechanism (Alrehaily *et al*. 2013):

$$Co^{2+} + OH^- \longrightarrow Co(OH)^+ \qquad \text{Equation 4(a)}$$

$$Co(OH)^+ + OH^- \longrightarrow Co(OH)_2 \qquad \text{Equation 4(b)}$$

$$Co(OH)_2 + OH^- \longrightarrow Co(OH)_3^- \qquad \text{Equation 4(c)}$$

$$4Co(OH)_2 + O_2 \longrightarrow 4CoOOH + 2H_2O \qquad \text{Equation 4(d)}$$

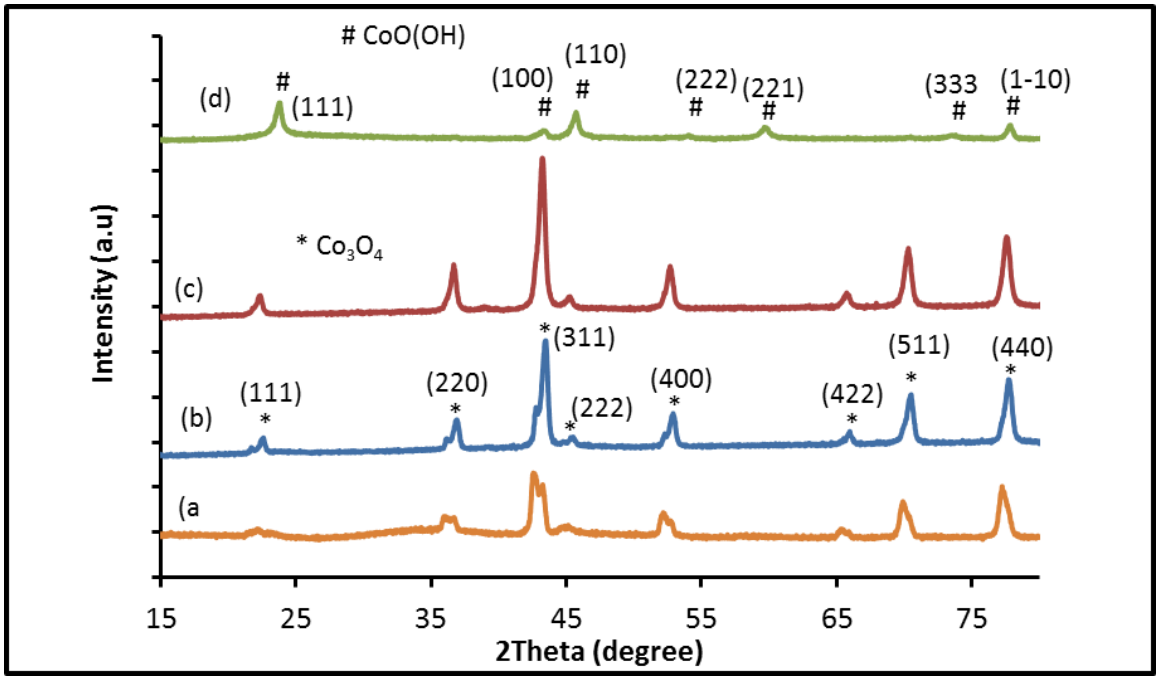

Figure 22: XRD pattern of cobalt oxide nanoparticles from (a) 0.2 M, (b) 0.3 M, (c) 0.4 M and (d) CoOOH particles synthesized from 0.7 M of NaOH.

3.4.4.2 Morphological of cobalt oxide nanoparticles synthesized at 0.2, 0.3, 0.4 and 0.7 M of sodium hydroxide

Figure 23 shows the morphology of the as-prepared of cobalt oxide nanoparticles from various concentrations of sodium hydroxide. The size distributions of the nanoparticles are shown in Figure 23 (b), (d) and (f). Due to mixed morphologies of particles obtained using 0.7 M of NaOH the size distribution could not be performed. The TEM images showed the cobalt oxide nanoparticles in cubic shape when 0.2, 0.3 and 0.4 M of NaOH was used while 0.7 M of NaOH showed a mixture of rods, sphere-like, cube- like and rectangular shapes. The particle sizes of 64.29 nm (standard deviation 21.97), 35.70 nm (standard deviation 23.44) and 28.54 nm (standard deviation 6.05) were obtained from synthesis using 0.2, 0.3 and 0.4 M of NaOH respectively. The size of the particles decreased as the concentration of NaOH increased from 0.2, 0.3 and 0.4 M. The size distribution of the particles from 0.4 M of NaOH had a narrower size distribution as compared to the 0.2 and 0.3 M of NaOH. The concentration of NaOH gives rise to a concentration of OH^- in solution, also referred to as ionic strength (Zhou *et al*. 2015, Xu & Zeng 2003) which allows for the precipitation to occur. This is, therefore, dependant on the pH.

Alleidene & Mohammed (2013) reported that at high pH particles tend to agglomerate due to the condensation of $Co(OH)_2$ and non-uniform particles also get formed. Different precipitation compounds and ionic strength might have been the cause of different shapes when 0.7 M of NaOH was used (Yang *et al*. 2007, Xu & Zeng 2003). Yun-Ling *et al*. (2013) indicated that at high concentration, excess OH^- aggregates on surfaces of certain particles which restrain the growth of the crystal surfaces because of repulsive interaction among OH^- ions which then lead to different shapes. At low concentration of NaOH there is less OH^-, because the repulsive force is small among OH^- ions and the concentration of hydroxyl is low in the reaction system.

The increased in NaOH concentration not only changed the phase of the nanoparticles (section 3.4.4.1) but also the size and shape of the particles.

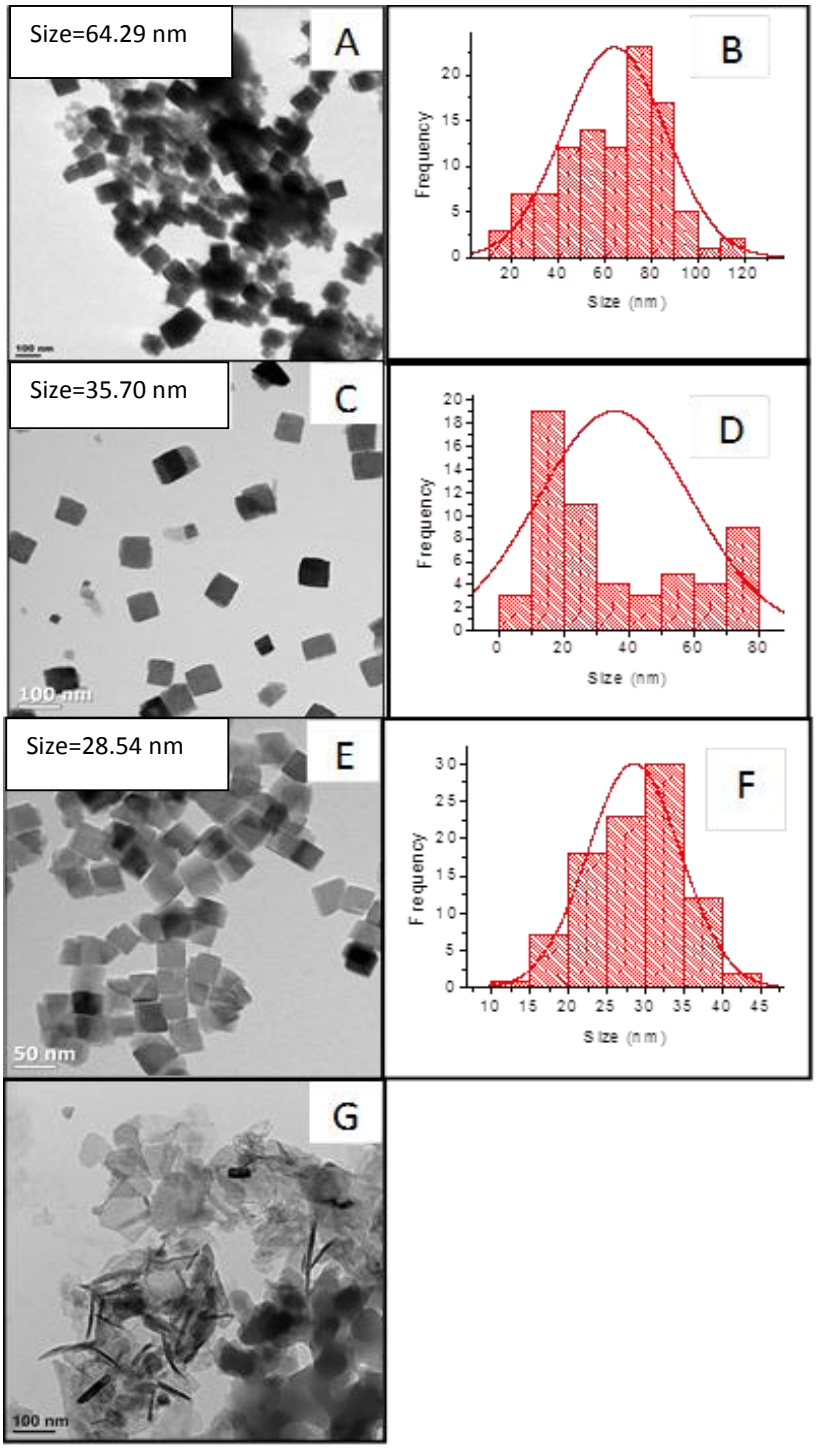

Figure 23: TEM images and size distribution of cobalt oxide nanoparticles synthesized from (a) 0.2 M, (c) 0.3 M (e) 0.4 M and (g) CoOOH synthesized from 0.7 M of NaOH.

3.4.4.3 FTIR spectroscopy of cobalt oxide nanoparticles synthesized at 0.2, 0.3, 0.4 and 0.7 M of sodium hydroxide

FTIR spectra of cobalt oxide nanoparticles prepared from NaOH concentrations of 0.2, 0.3, 0.4 and 0.7 M are shown in Figure 24. The broad peaks at 3441 cm^{-1} were due to the O-H stretch from all samples. The nanoparticles prepared from 0.2 M of NaOH showed the asymmetric CH_2 stretch at 2936 cm^{-1} and symmetric stretch at 2893 cm^{-1} which were not observed from other samples. This suggested that there was insufficient NaOH amount to completely convert the reactants to products hence the carbonyl, C=O stretch at 1740 cm^{-1} was observed. The nanoparticles prepared from 0.7 M of NaOH had peaks at 3433 and 1634 cm^{-1} due to O-H stretch and H-OH due to water molecules respectively. The asymmetric and symmetric COO^- was observed at 1585 and 1417 cm^{-1} respectively. The CoOOH particles seemed not to show the asymmetric and symmetric COO^-. This was expected because these particles had a different phase and not a Co_3O_4 as observed in the XRD results. This might due to precipitation composition of cobalt hydroxide (You-ping *et al*. 2007).

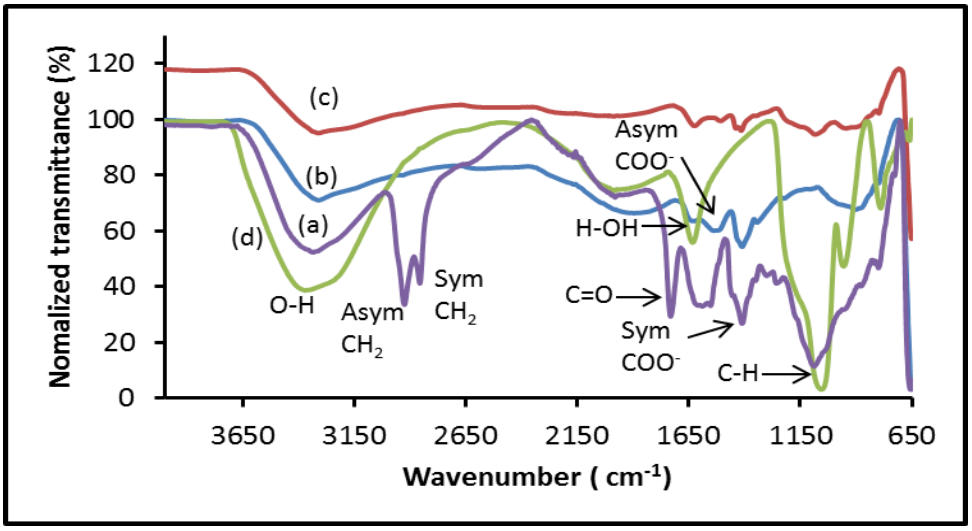

Figure 24: FTIR spectra of cobalt oxide nanoparticles synthesized from (a) 0.2 M, (b) 0.3 M, (c) 0.4 M and (d) CoOOH synthesized from 0.7 M of NaOH.

3.4.4.4 Optical properties of cobalt oxide nanoparticles at 0.2, 0.3, 0.4 and 0.7 M of sodium hydroxide

UV-vis and PL spectra of cobalt oxide nanoparticles prepared varying the concentration of sodium hydroxide are shown in Figure 25A and B respectively. All samples had multiple absorption peaks. The nanoparticles from 0.2 M of NaOH had absorption peaks at 245, 465 and 740 nm whilst the particles from 0.3 M of NaOH had peaks at 285, 459, 738 nm. The absorption peaks of nanoparticles synthesized with 0.4 M of NaOH were at 245, 460, 745 nm whilst 0.7 M of NaOH allowed the formation of CoOOH nanoparticles possessing their absorption peaks at 255, 420 nm. Only two peaks were observed for CoOOH which showed that a different path of reaction took place. The emission wavelengths were located at 773, 777, 768 and 776 nm for the samples with NaOH concentrations of 0.2, 0.3, 0.4 and 0.7 M respectively. The emission peaks were observed in the similar region.

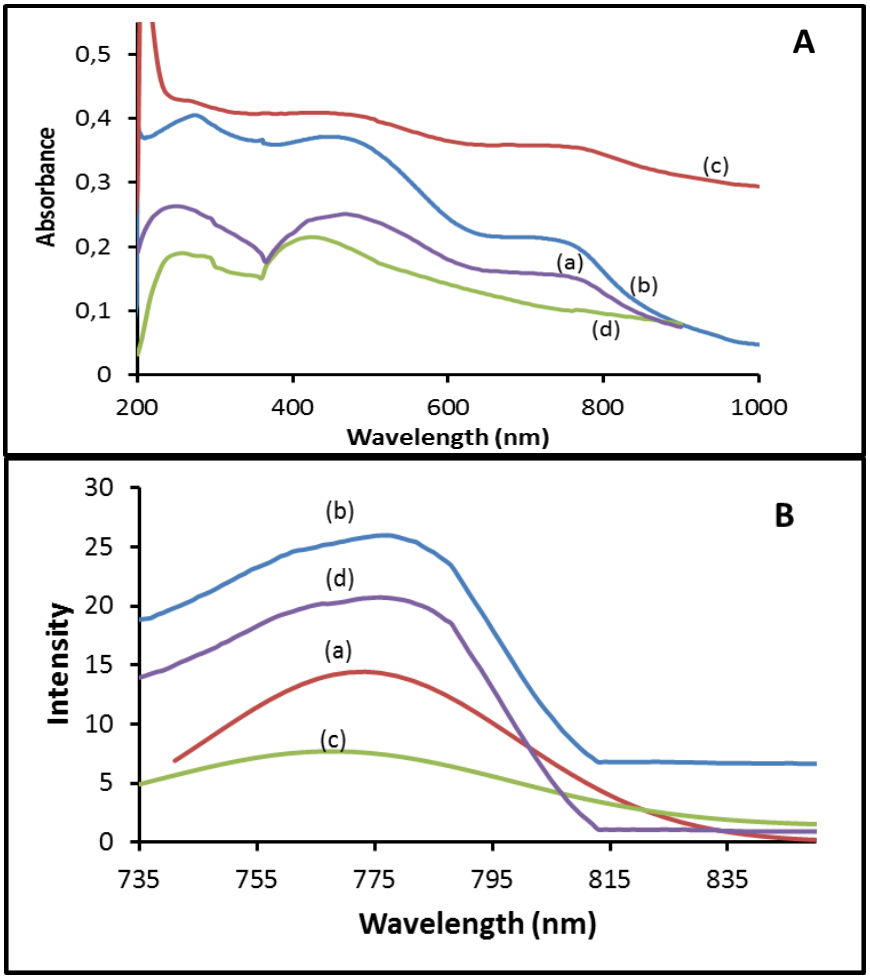

Figure 25: Absorption (A) and emission (B) spectra of cobalt oxide nanoparticles synthesized from (a) 0.2 M, (b) 0.3 M, (c) 0.4 M and (d) CoOOH synthesized from 0.7 M of NaOH.

3.4.5 Effect of capping molecule (acetic acid) on the synthesis of cobalt oxide nanoparticles

Cobalt oxide nanoparticles were prepared using cobalt nitrate and cobalt acetate as precursors, oxygen as oxidant and 0.7 M NaOH as a precipitating agent. A higher concentration of NaOH was used in order to neutralize and maintain the pH. Except cobalt acetate, cobalt nitrate was chosen as a different precursor which does not contain the carboxylic group. Therefore, the

nitrate group was compared with the acetate group in the presence acetic acid. Acetic acid (2.4 g used in order to obtain the same mole amount of Co^{2+}) was used as the shortest carboxylic acid to play a role of capping the nanoparticles.

3.4.5.1 X-ray diffraction of cobalt oxide nanoparticles capped with acetic acid from $Co(CH_3COO)_2$ and $Co(NO_3)_2$ precursors

The XRD pattern of the obtained cobalt oxide nanoparticles using cobalt acetate and cobalt nitrate in presence of acetic acid are shown in Figure 26. The spectra showed the diffraction pattern with indices of (111), (220), (311), (222), (400), (422), (511) and (440) corresponding to JCPDS number 03-065-1303 indexed to face-centered cubic phase (fcc**)** of cobalt oxide. The diffraction peaks of the nanoparticles synthesized from cobalt acetate were sharper compared to the nanoparticles from cobalt nitrate. This meant that the nanoparticles had high crystallinity. The use of acetic acid together with cobalt acetate gave the nanoparticles which showed narrow peaks compared to the synthesized nanoparticles in the absence of acetic acid (section 3.4.1.1). This suggested that the crystallinity of cobalt oxide nanoparticles improved with the adding of a capping agent. Moreover, due to the presence of acetic acid, the structural phase transformation from hexagonal CoOOH to fcc cobalt oxide (Co_3O_4) was effective.

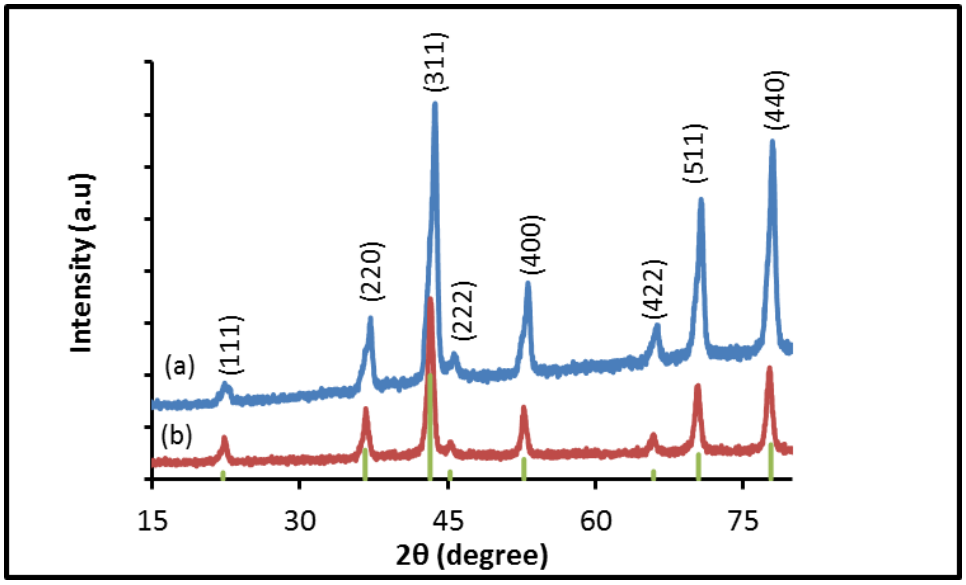

Figure 26: XRD patterns of cobalt oxide nanoparticles capped with acetic acid synthesized from (a) cobalt nitrate and (b) cobalt acetate precursors. The bars indicate the reference pattern of cobalt oxide (JCPDS number 03-065-1303).

3.4.5.2 Morphological of cobalt oxide nanoparticles capped with acetic acid from $Co(CH_3COO)_2$ and $Co(NO_3)_2$ precursors

The morphology and size distribution of cobalt oxide nanoparticles prepared from cobalt acetate and cobalt nitrate in the presence of acetic acid are shown in Figure 27. TEM images showed that the cubic shape of cobalt oxide nanoparticles capped with acetic acid was found in all both samples. The size distributions of the nanocubes are shown in Figure 26 (b) and (d) and the average sizes were 40.04 nm (standard deviation 11.43) and 33.31 nm (standard deviation 7.25) for acetic acid-capped nanocubes prepared from cobalt nitrate and cobalt acetate precursors respectively. The decrease in size was due to acetate group on the surface of the particles which indicated that the anion type played a role which was also evident on the effect of precursor (section 3.4.1.2). The morphological transformation was also observed. Cobalt nitrate yielded spherical-like nanoparticles whilst the addition of acetic acid allowed for

the formation of cubic nanoparticles. The average sizes of the nanoparticles prepared from cobalt acetate were smaller with a larger population compared to the nanoparticles synthesized from cobalt nitrate. Kusrini *et al*. 2015 showed that acetic acid formed better chitosan nanoparticles compared to lactic acid and formic acid.

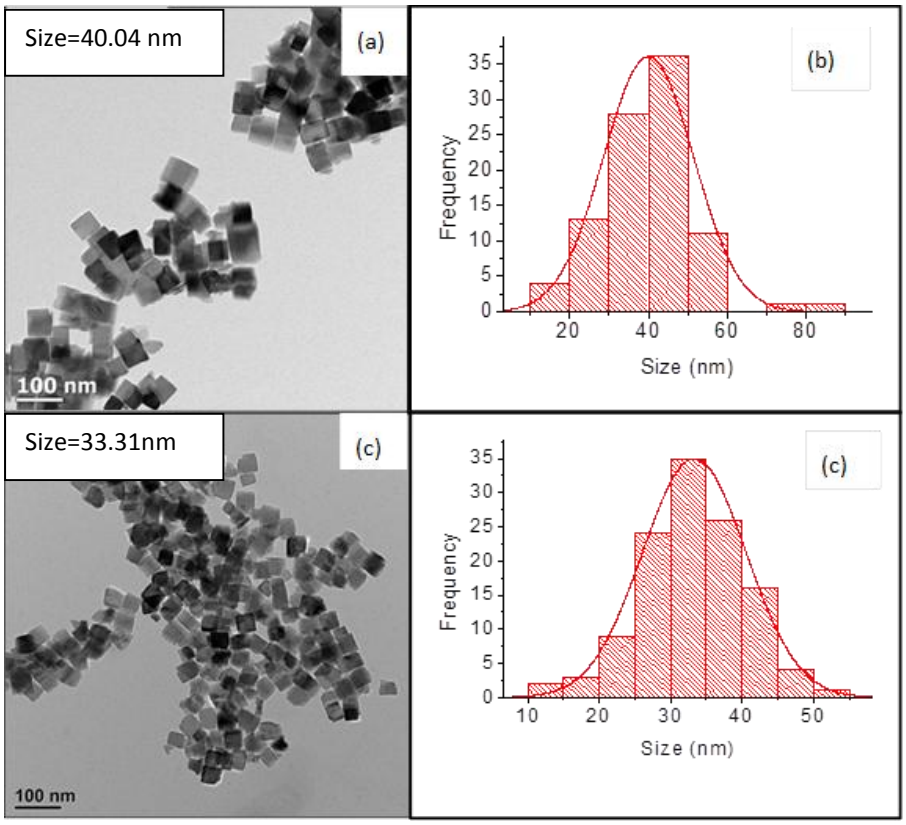

Figure 27: TEM images and size distribution of cobalt oxide nanoparticles capped with acetic acid synthesized from (a) and (b) cobalt nitrate, (c) and (d) cobalt acetate.

3.4.5.3 FTIR spectroscopy of cobalt oxide nanoparticles capped with acetic acid from $Co(CH_3COO)_2$ and $Co(NO_3)_2$ precursors

The FTIR spectra of Co_3O_4 nanocubes using cobalt acetate and cobalt nitrate in the presence of acetic acid are shown in Figure 28. The broad peaks at 3300 cm^{-1} were assigned to the O-H groups. The bands at 1632 cm^{-1} were due to H-O-H bending vibration. The asymmetric COO^- stretch at 1530 cm^{-1} and symmetric COO^- stretch at 1419 cm^{-1} was observed from both precursors. The asymmetric and symmetric COO^- peaks from nanoparticles prepared from cobalt nitrate were clearly visible as compared to the synthesis without the capping molecule (section 3.4.1.3). A shift to a lower frequency of the asymmetric and symmetric COO^- peaks from nanoparticles prepared from cobalt acetate was observed. There was no presence of the C=O group which proved that all the reactants had reacted and new COO^- peaks were formed. The use of acetic acid indicated that it was interacting strongly with the nanoparticles. The capping group was binding to the surface of the particles and forming a monolayer, therefore, forming a stable protective layer (Alledini & Muhammed 2013).

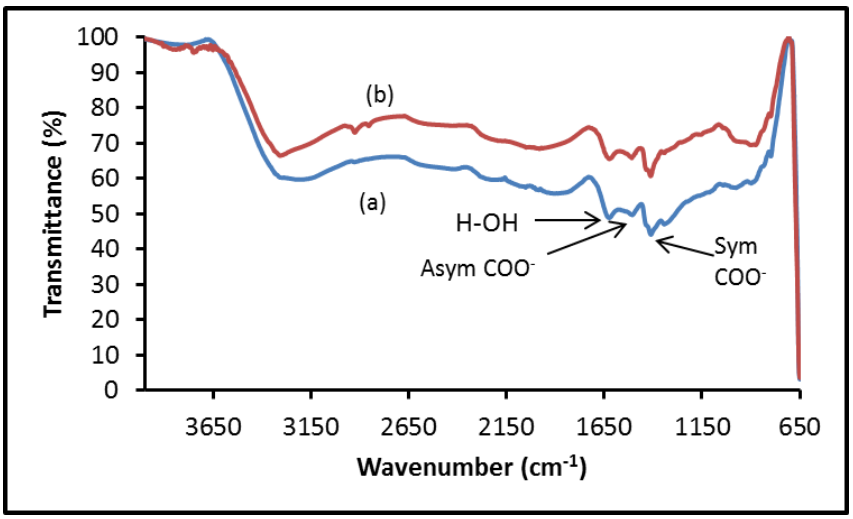

Figure 28: FTIR spectra of Co_3O_4 nanoparticles capped with acetic acid synthesized from (a) cobalt nitrate and (b) cobalt acetate.

3.4.5.4 Optical properties of Co_3O_4 nanoparticles capped with acetic acid from $Co(CH_3COO)_2$ and $Co(NO_3)_2$ precursors

The optical properties of the obtained cobalt oxide nanoparticles using cobalt acetate and cobalt nitrate capped with acetic acid are shown in Figure 29. The absorption wavelengths (Figure A) for nanoparticles prepared from cobalt nitrate were 239, 412 and 715 nm, whilst the nanoparticles from cobalt acetate had their absorptions at 205, 316 and 675 nm.

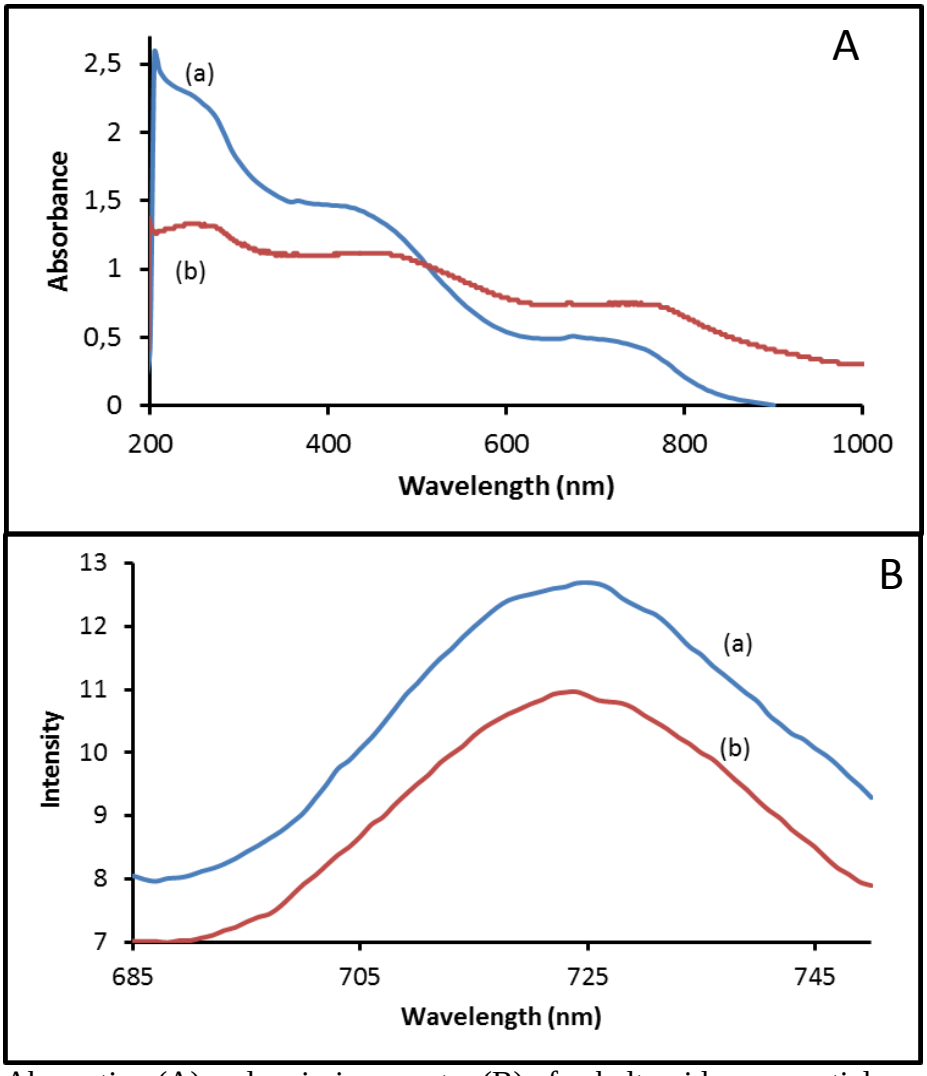

Figure 29: Absorption (A) and emission spectra (B) of cobalt oxide nanoparticles capped with acetic acid synthesized from (a) cobalt nitrate and (b) cobalt acetate.

The absorption wavelength of the nanoparticles using cobalt acetate was blue shifted compared to nanoparticles from cobalt nitrate which is in agreement with the TEM results. The blue shift of the nanocubes from cobalt acetate showed that the acetate group from the acid and the precursor played an important role in reducing the particles size. The capped nanoparticles from both precursors were smaller compared to the uncapped (section 3.4.1.2) nanoparticles which showed that the use of acetic acid played a role in controlling the growth of cobalt oxide nanocubes. The photoluminescence spectra are shown in Figure 29B. The emission peak of cobalt oxide nanoparticles was 720 nm from both precursors. The PL of the capped nanoparticles from both precursors was blue shifted compared to the uncapped nanoparticles. This indicated that the capped nanoparticles from both precursors were smaller as compared to the uncapped particles. The acetate was competing with the nitrate ion when cobalt nitrate was used. This in turn was responsible for size reduction and changed in morphology when cobalt nitrate was used. The formation of cubic morphology might have been due to the use of acetic acid as a capping molecule. The precipitation composition of sodium hydroxide was enough to form $Co(OH)_2$ or $Co(OH)_3$, this might led to nitrate and the acetate to form part of the precipitation composition (Viljoen *et al*. 2017) The acetic acid assisted in forming the same precipitation composition hence the formation of cobalt oxide nanocubes.

References

ABDELRAZEK, E. M. & ELASHMAWI, I.S. 2008. Characterization and physical properties of $CoCl_2$ filled polyethyl-methacrylate films. *Wiley Inter Science*. 6, 1036-1043.

ALLAEDINI, G. & MUHAMMAD, A., 2013. Synthesis and characterization of cobalt oxide nanoparticles. *Journal of Nanostructure in Chemistry,* 3, 1-16.

ALREHAILY, L.M., JOSEPH, J.M., BIESINGER, M.C., GUZONASC, D.A. & J. C. WREN. 2013. Gamma-radiolysis-assisted cobalt oxide nanoparticle formation. *Journal of Physical Chemistry,* 15, 1014-1024.

BHATT, A.S., BHAT, D.K., TAI, C. & SANTOSH, M.S. 2011. Microwave-assisted synthesis and magnetic studies of cobalt oxide nanoparticles. *Materials Chemistry and Physics*, 125. 347-350.

CASILLA, P.E.G., GONZELAS, C.A.R. & PEREZ, C.A.M. 2012. Infrared spectroscopy of functionalized magnetic nanoparticles. *Material Science, Engineering and Technology*. 405-13, 417.

CUI, H., ZHAO, Y., REN, W., LIU, Y. & WANG, M. 2013. Aqueous foams stabilized solely by CoOOH nanoparticles and the resulting construction of hierarchically hollow structure. *Journal Nanoparticle Research*. 15.1851-1857.

VILJOEN E. L., MOLOTO, M.J., THABEDE, P.M. 2017. Impact of acetate ions on the shape of Co_3O_4 nanoparticles. *Digest Journal of Nanomaterials and Biostructures*, 12, 571-577.

FENG, J. & ZENG, H.C. 2003. Size-controlled growth of Co_3O_4 nanocubes**.** *Chemical of Material, 15,* 2829-2835.

HE, T., CHEN, D., JIAO, X., WANG, Y. & DUAN, Y. 2005. Solubility-controlled synthesis of high-quality Co_3O_4 nanocrystals. *Chemical of Materials,* 17, 4023-4030.

KANG, M. & ZHOU, H. 2015. Facile synthesis and structural characterization of Co_3O_4 nanocubes. *AIMS Materials Science* 2, 16-27.

KODGE, A., KALYANI, S. & LAGASHETTY, A. 2011. Microwave preparation, characterisation and studies of nanosized cobalt oxide. *International Journal of Engineering Science and Technology*, 3, 6381-6389.

KUSRINI, E., SHIONG, S., HARAHAP, Y., YULIZAR, Y., ARBIANTI1, R. D. & PUDJIASTUTI, A.R. 2015. Effects of monocarboxylic acids and potassium persulfate on preparation of chitosan nanoparticles. *International Journal of Technology*, 1, 11-21.

LEY, A. 2009. A spectroscopic and thermal study of cobalt carboxylates. University of the Witwatersrand, A dissertation submitted to the Faculty of Science, University of the Witwatersrand, in fulfillment of the requirements for the degree of Master of Science, 1-121

LIU, X., QIU, G. & LI, X. 2005. Shape-controlled synthesis and properties of uniform spinel cobalt oxide nanocubes. *Nanotechnology,* 16, 3035-3040.

NIASARI, M.S., MIR , N. & DAVAR, F. 2009. Synthesis and characterization of Co_3O_4 nanorods by thermal decomposition of cobalt oxalate, *Journal of Physics and Chemistry of Solids.* 70: 847-852.

SCHNELLER, T., WASER, R., KOSEC, M. & PAYNE, D. 2013. Chemical solution deposition of functional oxide thin films. *Springer-Verlag Wein*, 29-49.

SPATARU, N., TERASHIMA, C., TOKUHIRO, K., SUTANTO, S., TRYK, D.A., PARK, S. & FUJISHIMA, A. 2003. Electrochemical Behavior of Cobalt Oxide Films Deposited at Conductive Diamond Electrodes. *Journal of the Electrochemical Society*, 150, E337-E341.

TENG, Y., YAMAMOTO, S., KUSANO, Y., AZUMA, M. & SHIMAKAWA, Y. 2010. One-pot hydrothermal synthesis of uniformly cubic Co_3O_4 nanocrystals. *Materials Letters*. 64, 239-242.

THOTA, S., KUMAR, A. & KUMAR, J. 2009. Optical, electrical and magnetic properties of Co_3O_4 nanocrystallites obtained by thermal decomposition of sol-gel derived oxalates. *Materials Science and Engineering* B, 164. 30-37.

WANG, W. & XU. J. 2015. Structure and visible light luminescence of 3D flower-like Co_3O_4 hierarchical microstructures assembled by hexagonal porous nanoplates. *ACS Applied Materials. Interfaces*, 7, 415-421.

WANG, J., NIU, B., DU, G., ZENG, R. CHENG, Z., GUO, Z. & DOU, Z. 2011. Microwave homogeneous synthesis of porous nanowire Co_3O_4 arrays with high capacity and rate capability for lithium ion batteries. *Materials Chemistry and Physics*, 126, 747-754.

YIN, M., WILLLIS, A., REDL, F., TURRO, N. J. & BRIEN, S. P. 2004. Influence of capping groups on the synthesis of ɣ-Fe_2O_3 nanoparticles. *Journal Materials Research,* 19, 1208-1214.

XU & ZENG, H.C. 2003 Mechanistic investigation on salt-mediated formation of free-standing Co_3O_4 nanocubes at 95 °C. *Journal of Physical Chemistry. B, 107,* 926-930.

YANG, Y-P., LIU, R-S., HUANG, K-L.,WANG, L-P., LIU, S-Q. & ZENG, W-W. 2007. Preparation and electrochemical performance of nanosized Co_3O_4 via hydrothermal method. *Transactions of Nonferrous Metals Society China*, 17, 1334-1338.

YUN-LING, L., JING-ZHE, Z., YAN, Z., XIN-L.I. & ZHEN-YU. 2013. Facile solution-based synthesis and optical properties of Co_3O_4 nanoparticles at low-temperature. Chemical Research China University, 29, 1040-1044.

ZHOU, L., WANG, S., MA, H., MA,S. & XU, D. *2015.* Size-controlled synthesis of copper nanoparticles in supercritical water. *Chemical Engineering Research and Design*, 98. 36-43.

CHAPTER 4: CONCLUSIONS AND RECOMMENDATIONS

4.1 Conclusions

Synthesis of cobalt oxide nanoparticles was conducted by decomposing cobalt carboxylates with different chain length using the microwave assistance method. The preparation of the nanoparticles from this method resulted into large particles. This might have due to high temperature used (200 °C). From the data collected, the difference in chain length of the carboxylic ligands had an influence on the size and shape of Co_3O_4 nanoparticles. The results showed that the prepared complexes were successfully formed, as observed from the elemental analysis except for the cobalt acetate. The TGA analysis showed that the decomposition temperature increases as the length of hydrocarbon chain of the complexes increases. The FTIR spectroscopy showed that COO^- peaks associated with the carboxylate and C=O stretch associated with the carboxylic acid was present in the complexes and the nanoparticles. This was due to insolubility of the cobalt complexes. XRD pattern showed that the particles were composed of cobalt-basic-carbonate and cobalt oxide phases.

The study of parameters showed that they had an influence on size and shape control of cobalt oxide particles**.** Physical parameters, shape, and size were controlled by the introduction and the absentia of the carboxylic group during the study of the acetate group. TEM showed that the size of the nanoparticles was smaller in the presence of the acetate group. The acetate played a role of a capping molecule by reducing the size of cobalt oxide nanoparticles. Not only did the acetate influence the size of the nanoparticles but also the morphology. FTIR spectra showed that the carboxylate group adsorbs on the surface of the nanoparticles. This suggested that the acetate was responsible for the reduction of the size of the nanoparticles. The

morphology and size of cobalt oxide nanoparticles were dependent on the anion type of the cobalt salts. The effect of oxidant using oxygen and hydrogen peroxide showed that hydrogen peroxide was able to reduce the size to smaller particles and had a narrow size distribution as compared to oxygen. Using different oxidants did not have an influence on the shape of cobalt oxide nanoparticles but rather on the size of the particles. A stronger oxidant (H_2O_2) produced smaller nanoparticles as compared to oxygen. UV-vis spectroscopy of nanoparticles synthesized using hydrogen peroxide was red-shifted as compared to nanoparticles prepared using oxygen which was due to faster reaction rate and defects on the surface of the nanoparticles. Increasing the duration of the synthesis also made the particles to increase in size. An increase in pH led to an increased in the ionic strength which had an influence on the size, morphology, and phase of cobalt oxide nanoparticles. TEM showed that the size of cobalt oxide nanocubes decreased with an increase of NaOH concentration. A further increase of NaOH concentration changed the morphology and phase of the particles to CoOOH. Using acetic acid as a capping molecule reduced the size of cobalt oxide nanoparticles as compared to an absence of acetic acid. Morphology of the particles also changed from spheres to cubes when cobalt nitrate was used as the precursor. Optical properties showed that the nanocubes from cobalt acetate were blue shifted as compared to particles from cobalt nitrate. This meant that the nanoparticles prepared from cobalt acetate were smaller in sizes.

Synthesis of nanoparticles using microwave-assisted method produced polydispersed particles due to insolubility and steric hindrance of the longer chain cobalt complexes. The chemical precipitation method gave nanoparticles with fcc phase of cobalt oxide and CoOOH when a high concentration of NaOH was used. Synthesized cobalt oxide can, therefore, be used for many applications such as photocatalysis, conductors, etc.

4.2 Recommendations

Cobalt oxide nanoparticles may not have been formed due to the absence of an oxidizing agent when using the microwave technique. It is therefore recommended that the synthesis of cobalt oxide nanoparticles be conducted in the presence of an oxidizing agent like hydrogen peroxide to enable the direct formation of cobalt oxide nanoparticles and assisting in obtaining small particles. Alternatively, a calcination step can be introduced after the microwave technique. However, calcination may result in larger particles forming due to sintering.